UNCLASSIFIED

SECURITY CLASSIFICATION OF THIS PAGE *(When Data Entered)*

DTIC FILE COPY

(1)

AD-A196 382

REPORT DOCUMENTATION PAGE

READ INSTRUCTIONS BEFORE COMPLETING FORM

1. REPORT NUMBER: AFIT/CI/NR 88- 77	2 GOVT ACCESSION NO.
3. RECIPIENT'S CATALOG NUMBER	
4. TITLE *(and Subtitle)*: CHARACTERIZATION OF METALLIC COATINGS AND THIN FILMS PRODUCED BY RAILGUN DEPOSITION	5. TYPE OF REPORT & PERIOD COVERED: MS THESIS
	6. PERFORMING ORG. REPORT NUMBER
AUTHOR(s): RUSSELL JOSEPH DELUCA	8. CONTRACT OR GRANT NUMBER(s)
PERFORMING ORGANIZATION NAME AND ADDRESS: AFIT STUDENT AT: UNIVERSITY OF TEXAS - AUSTIN	10. PROGRAM ELEMENT, PROJECT, TASK AREA & WORK UNIT NUMBERS
CONTROLLING OFFICE NAME AND ADDRESS	12. REPORT DATE: 1988
	13. NUMBER OF PAGES: 94
MONITORING AGENCY NAME & ADDRESS *(If different from Controlling Office)*: AFIT/NR, Wright-Patterson AFB OH 45433-6583	15. SECURITY CLASS. *(of this report)*: UNCLASSIFIED
	15a. DECLASSIFICATION/DOWNGRADING SCHEDULE

16. DISTRIBUTION STATEMENT *(of this Report)*

DISTRIBUTED UNLIMITED: APPROVED FOR PUBLIC RELEASE

DTIC ELECTE AUG 0 3 1988 S D H

17. DISTRIBUTION STATEMENT *(of the abstract entered in Block 20, If different from Report)*

SAME AS REPORT

18. SUPPLEMENTARY NOTES

Approved for Public Release: IAW AFR 190-1
LYNN E. WOLAVER Lynn Wolaver 19 July 88
Dean for Research and Professional Development
Air Force Institute of Technology
Wright-Patterson AFB OH 45433-6583

19. KEY WORDS *(Continue on reverse side if necessary and identify by block number)*

20. ABSTRACT *(Continue on reverse side if necessary and identify by block number)*

ATTACHED

DD FORM 1 JAN 73 1473 EDITION OF 1 NOV 65 IS OBSOLETE

UNCLASSIFIED

SECURITY CLASSIFICATION OF THIS PAGE *(When Data Entered)*

ABSTRACT

CHARACTERIZATION OF METALLIC COATINGS AND THIN FILMS PRODUCED BY RAILGUN DEPOSITION

by

Russell Joseph DeLuca
Captain, USAF

1987

Thesis, 104 pages.

Degree Awarded: Master of Science in Engineering

The University of Texas, Austin

This project was an investigative and exploratory study into the use of a "Railgun" material accelerator as a deposition tool. The railgun system was powered by new technology quick pulse capacitance discharge banks. These banks were capable of discharging up to 35 kJ of energy in less than 100 microseconds. Given such an energetic process, the goal was to produce unique depositions, and novel materials or coatings not readily produced by other commercial techniques.

The study included over 150 discharges of the open bore railgun employing some 15 different metallic material systems. In addition, the machine hardware was modified for improvement throughout the entire investigation. In the systems final configuration, it was capable of producing two distinct types of depositions, relatively thick deposits with a graded structure, and very thin metallic films with a uniform structure. The latter, production of thin films by railgun deposition, is a new evolutionary technique.

In either configuration, material system mixing is possible in the liquid , vapor , and plasma state. This mixing technique can be used to

produce intermetallic phases or varying composition alloys. Additionally, promise was shown for the production of metastable non-crystalline and non-equilibrium states. The gun's capability to match the micro - scale structure of the new rapid solidification (RS) technology is also indicated. Lastly, the railgun was shown capable of substantial surface modification as the plasma arc was traveling at speeds as high as 40 km / sec.

BIBLIOGRAPHY

PRIMARY SOURCES

1. Bunshah, R. F., Deposition Technologies for Films and Coatings ,Noyes Publications, New Jersey. 1982.

2. Glang, R., Handbook of Thin Film Technology, McGraw Hill Inc. 1970.

3. Spann, M. L., Brown, L. D., "Formation of Amorphous Metal by Hypervelocity Impact," EL-3238, Research Project 2115-6, Final Report, Oct 83, University of Texas, Austin.

4. Proceedings of the 3rd. Symposium on Electromagnetic Launch Technology '86, held in Austin TX. April 1986 IEEE Transactions on Magnetics, Vol. Mag-23, Nov. 1986.

5. Barber, J. P., Marshall, R. A., Rashleigh, S., "Magnetic Propulsion for a Hypervelocity Launcher," J. Appl. Phys. Vol. 49, 4 (April 1978) p. 2540.

6. Brast, D. E. and Sawle. D. R., "Feasibility Study for Development of a Hyper Velocity Gun," NASA-CR-60119 (1964).

7. Barber, J.P., "The Acceleration of Macroparticles in a Hypervelocity Electromagnetic Accelerator," Ph.D. Thesis, The Department of Engineering Physics, Australian National University, Canberra, Australia (1972).

8. Hawk, R. S., Scudder, J. K., "Magnetic Propulsion Railguns: Their Design and Capabilities," in Megagauss Physics and Technology, ed. P. J. Turchi, Proceedings of an Int. Conf. on Megagauss Magnetic Field Generation and Related Topics, Washington, D. C. 1979.

9. Marshall, R.A., "Moving Contacts in Macro-Particle Accelerators", in High Power-High Energy Pulse Production and Application, ed. E.K. Inall, Australian National University Press, (Canberra) 1978.

CHARACTERIZATION OF METALLIC COATINGS AND THIN FILMS

PRODUCED BY RAILGUN DEPOSITION

APPROVED:

DEDICATION

To my lovely wife, Kathye Jo DeLuca, for her understanding and support throughout this endeavor.

CHARACTERIZATION OF METALLIC COATINGS AND THIN FILMS PRODUCED BY RAILGUN DEPOSITION

by

RUSSELL JOSEPH DELUCA, B.S.

THESIS

Presented to the Faculty of the Graduate School of

The University of Texas at Austin

in Partial Fulfillment

of the Requirements

for the Degree of

MASTER OF SCIENCE IN ENGINEERING

THE UNIVERSITY OF TEXAS AT AUSTIN

MAY, 1987

ACKNOWLEDGMENTS

I would like to thank Dr. Harris L. Marcus, first, for giving me the opportunity to work on this project, and second, for his guidance and support throughout. Additionally, I thank Dr. Zwy Eliezer for his project advice, and especially the technical critique of this manuscript. To Dr. Chadee Persad, I extend a special thanks for his daily direction and counsel. As others contributed significantly to this project, I would also like to acknowledge their contribution. I greatly appreciated the help of Dr. Llewellyn Rabenberg, Dr. Michael Schmerling, and Dr Steve Swinnea with the TEM, SEM, and X-Ray diffraction work. My gratitude goes out to the CEM staff, especially to Dennis Peterson for his conceptual guidance on Railgun Technology, and to both Marv House and Jim Allen for their technical assistance. Finally, to the graduate students, especially Chris Lund and Rick Barrera, a little help goes a long way, thanks, and good luck in the future.

This research was partially supported by DARPA under NADC contract, N62269-85-C-0222.

ABSTRACT

This project was an investigative and exploratory study into the use of a Railgun material accelerator as a deposition tool. The railgun system was powered by new technology quick pulse capacitance discharge banks. These banks were capable of discharging up to 35 kJ of energy in less than 100 microseconds. Given such an energetic process, the goal was to produce unique depositions, and novel materials or coatings not readily produced by other commercial techniques.

The study included over 150 discharges of the open bore railgun employing some 15 different metallic material systems. In addition, the machine hardware was modified for improvement throughout the entire investigation. In the system's final configuration, it was capable of producing two distinct types of depositions, relatively thick deposits with a graded structure, and very thin metallic films with a uniform structure. The latter, production of thin films by railgun deposition, is a new evolutionary technique.

In either configuration, material system mixing is possible in the liquid , vapor , and plasma state. This mixing technique can be used to produce intermetallic phases or varying composition alloys. Additionally, promise was shown for the production of metastable non-crystalline and non-equilibrium states. The gun's capability to match the micro - scale structure of the new rapid solidification (RS) technology is also indicated. Lastly, the railgun was shown capable of substantial surface modification as the plasma arc was traveling at speeds as high as 40 km / sec.

The success and knowledge gained through this study has also opened the

door for some future worthwhile efforts. The details of the deposition / substrate interaction must first be studied in depth, and then this process can be tailored for specific material research.

TABLE OF CONTENTS

LIST OF FIGURES

CHAPTER 1

INTRODUCTION

The idea of coating a surface with a different material dates back to the beginning of advanced civilization. What is interesting is that the early reason, to improve some property, has not changed with time but just advanced in degree. Today as an example, we are propelling ions at relativistic speeds to dope electronic devices, make impervious atomic barriers, and to improve surface wear properties. However, like our ancestors, we are still coating for artistic reasons. The current application for coatings or thin films can then be broken down into roughly five generic categories. These categories are optical, electrical, mechanical, or chemical property improvement, as well as for decorative reasons. (1)

As there are numerous reasons for coating or laying down thin films, there are nearly an equal number of different technologies currently available to complete the task. There is no one definitive technique, but each has its own advantages, disadvantages, and realm of operation. Perhaps the first documented production of thin films dates back to Faraday and Nahrwold in the late 1800's. These men successfully evaporated and deposited metal films by Joule heating of thin wires. (2) Likewise, chemical reduction and spraying processes for thicker coatings date back as far. The first plasma generator was created by Gerdien in 1922. (3) Despite their lead, these advances were slow to mature and commercially missed due to the lack of control, inadequate power supplies, and the absence of good vacuum systems. (2) However, in the last 30 years, all of these requirements

have been met, and the various technologies have bloomed. Surprisingly though, our apparent needs are now keeping pace if not driving the coating and thin film production technology. That is, todays technology is such that materials are being employed to and beyond their limit. Thereby, we still need new and better means of fulfilling the coating and thin film application categories.

Zaat, in his quarter century review of plasma spraying, clearly indicated the need of a plasma source which would have the momentum to assure intensive contact during impact. (3) As a result of this lack of good contact, a post treatment like annealing is often used. On the other hand, thin film technologies, have their own merits and vices. Sputtering and evaporation techniques are today very capable and well controlled. They have been shown to produce consistent, unique, and metastable films. Yet, these processes are very time consuming, and the films often show preferred crystallographic orientation. This may or may not be a desired property. At the high end of the energy scale, ion implanters (4) have favorably improved the surface properties of many materials. This is however, really a subsurface technique. The surface properties are changed by what is driven just below. The technique generally produces a distribution of implanted ions with the maximum at a depth which is both ion energy and material specific. Control of this process is now coming into its own. The latest associated technique has been ion mixing (5). This technique involves depositing a thin surface film, and then driving it into the substrate with high energy ions for the desired effect. Unfortunately, with such energetic ions, sputtering and lattice damage occurs. Once again, a post treatment is used to mitigate or alleviate these undesirable consequences. (5)

The application of electromagnetic propulsion (6) to form coatings may fill some voids in our present technology. It also offers the means to highly

accelerate a plasma once generated.

RAILGUN CONCEPT

Historically, the concept of electromagnetic propulsion was proposed in the early 1800's when Oersted and Ampere first worked with the laws of electro-motion. (7) More recently, engineers and physicists in the late 1950's and early 1960's were experimenting with these concepts to develop a pulsed rocket engine for space travel. (8) This idea soon lost impetus due in part to the lack of an adequate power supply on a weight basis. However, over the last 15 years, there has been a definite advancement in pulsed power sources. These new power devices, capacitance discharge banks (9), homopolar generators (10), and compensating alternators (11) are capable of delivering megajoules of energy in less than a second. This advancement has opened the door for numerous applied research possibilities. (12) Electromagnetic accelerators, "railguns" , (7,10) have seemingly emerged as the mainstay for their use. These railguns are being investigated for propulsion of projectiles to hypervelocities (above 10 km / sec). (12) What is interesting is that these projectiles are often driven electromagnetically by plasma arcs. The plasma is generated by vaporization of conductive metals. A typical plasma armature involves approximately 10 mg of material. If this 10 mg armature was traveling at 10 km / sec, it would contain 500 joules of kinetic energy by calculation. Now, if this energy was distributed evenly among the ions, their individual energy would be on the order of 10 - 100 eV. Figure 1 graphically displays the relation of this plasma source with other directed energy beams used for deposition.

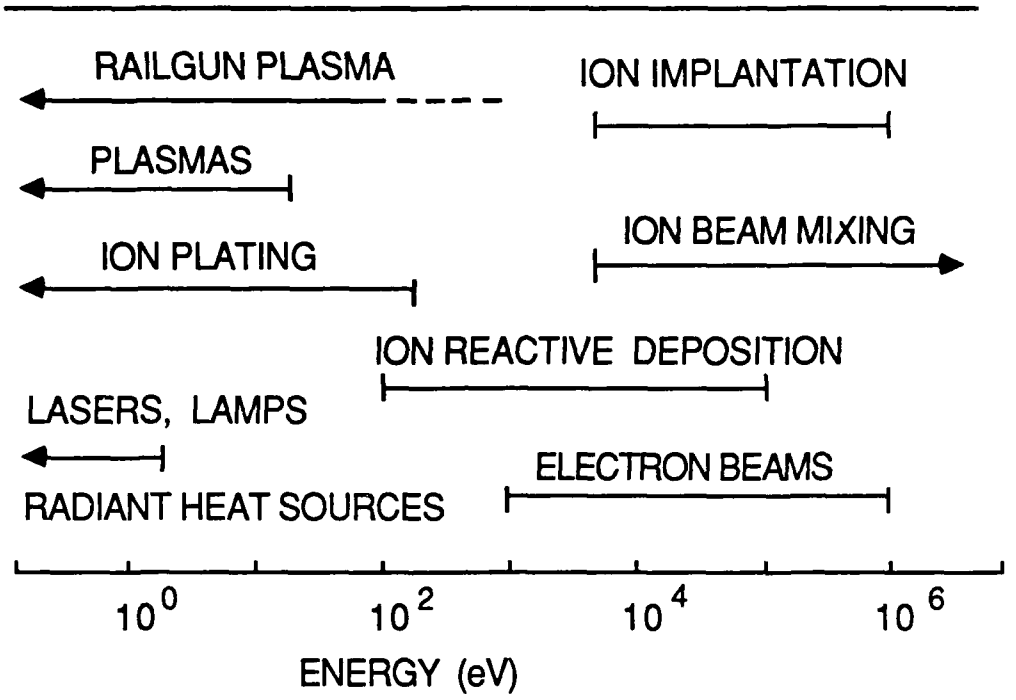

Figure 1 : Directed Energy Beams

Barber gives an excellent description of railgun operation. (7) A railgun is simply a DC motor which consists of two rigid parallel conducting electrodes (rails) and a combined movable armature placed between them (7), Figure 2. The armature can be in any physical state, that is solid, liquid, vapor or plasma (13). The armature sometimes undergoes a progressive change of state . This is the case when fused metallic foils are used as the generating source of plasma for the armature. Schematically, current flows from the power source, to the top rail, across the armature, and back out the bottom rail. This flowing current develops a magnetic field between the rails. The magnetic field then exerts a pressure or force on the back of the armature. This force, known as the Lorentz force, becomes very large at

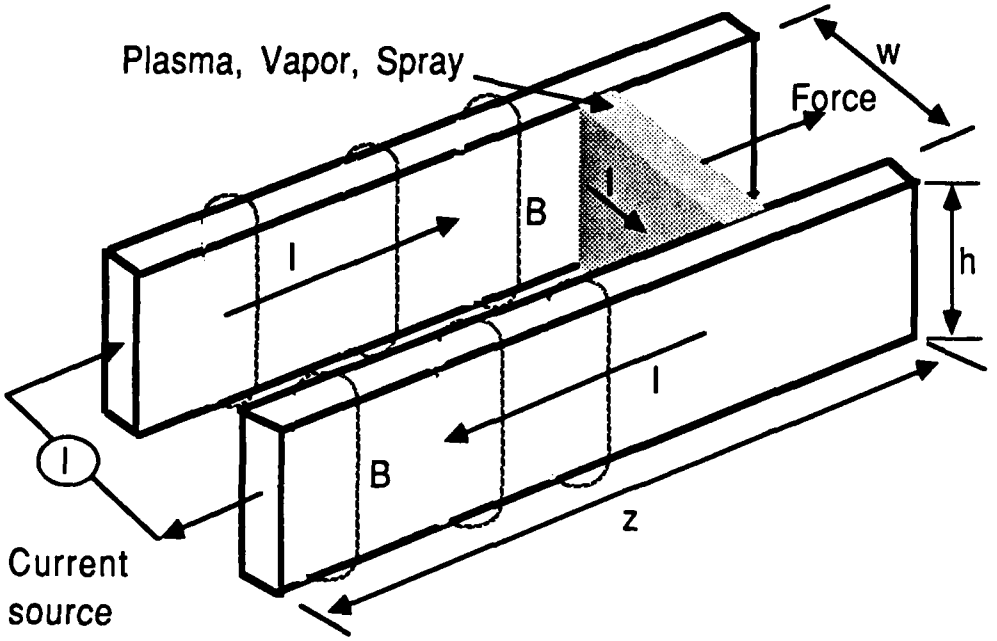

Figure 2 : Railgun Concept

high currents. (8) Quantitatively,

$$F = L_1 I^2 / 2$$

where F is the force, I is the armature current, and L_1 is the inductance per unit length of the rails. For an armature of mass m, the acceleration is

$$a = L_1 I^2 / 2 m .$$

The above equations indicate that for a one meter railgun with $L_1 = 0.5$ uH / m , a current of 1 MA would produce an acceleration of 10^6 - 10^7 m / sec^2 on a 1g

armature. (7) Based upon this calculation, the hypervelocity regime for a plasma arc is attainable. Therein lies the promise of the railgun for deposition purposes.

RAILGUN DEPOSITION

As previously noted, deposition by plasma source is already a commercial tool; however, the concept of using a railgun to accelerate the plasma during the deposition process is very new. In fact, the literature on this topic is most limited, especially in the free world. Two groups, one in Poland(14) and one in Russia(15) have published papers dealing with pulsed power and gas injected railguns for deposition. The earliest reference to this topic that the author was able to find was a related conference presentation by Lau and Margerun in 1976. (16) Their presentation covered the possibility of using pulsed plasma acceleration with thermal spraying. Since that presentation, The Center for Electromechanics (CEM) at Balconies Research Center, University of Texas, and NASA have completed the only investigations of this process in the free world.

The first investigation was conducted by Brown (17) and Spann and Brown (18) in 1983. They successfully used a railgun to deposit an iron based metglas on room temperature and chilled (100K) stainless steel or copper substrates. Their efforts were aimed at building up, by multi-shot, a thick amorphous deposit for possible use in transformer cores. These deposits were subsequently characterized as having retained various degrees of non-crystallinity. They concluded that deposition by this technique in the glass state was possible and promising; however, their success was limited to approximately a 40 μm thick, layered deposit , with 10% crystalline structure. The deposits were also found to be irregular in both

consistency and microstructure, and appeared to have been formed by liquid splatting. Additionally, no amorphous deposits were made from crystalline material.

With regards to their experimental set up, an 80 cm square bore railgun was used. This railgun was powered by a quick pulse capacitance discharge bank capable of delivering approximately 100 kA at low voltage. The experiments were conducted in light vacuum, 10^{-1} Torr. The railgun was charged by placing either wire or ribbon foil across the rails in various configurations. Sabots holding powders were also used unsuccessfully in an attempt to generate a movable armature. In any case, their armatures of mixed liquid and plasma were created by joule heating of material (primarily foils) packed between the rails. As a consequence, a large portion of the energy available went into creating the arc.

Based upon the results of Brown and Spann, CEM has since completed two additional year long engineering studies involving the application of railgun technology to surface coating. (19)

The first additional study involved the deposition of stainless steel on mild steel substrates for corrosion resistance. The experimental setup was almost identical to that of Brown's. Once again foils were spring loaded between the rails, and various unsuccessful configurations with powders were attempted. However, their setup did include magnetic probes for the determination of plasma velocity. This study concluded that railgun deposition is effective. The coated substrates did show superior corrosion resistance. Additionally, results from oscilloscope traces indicated the armature was traveling between 5 -10 km / sec, and that it consisted of multiple arcs. Coatings were again characterized as a build up of overlapping lenticular and globular splats. The deposited weight efficiency was found to be 20%, and thickness ranged to 175 μm after multi-shot. Iron oxides were found and

attributed to the opening of the light vacuum chamber after each discharge. Finally, the idea of automatic wire or foil feeding was presented to preclude breaking vacuum.

The second study began with single shot exploding wire and ribbon experiments in vacuum (1×10^{-3} Torr). These wires or ribbons were made from either iron or cobalt based metglas. Capacitance discharge was used to explode the materials. Peak currents reached 190 kA at approximately 1.5 μsec. Electrical potential was also used in an attempt to drive the exploding products onto targets. These targets were placed in several different geometric positions close to the exploding wires or ribbons. The obtained deposits were very thin, and could easily be wiped off the substrate with tissue.

Further efforts included the addition of an automatic wire or foil feeder to preclude breaking vacuum as conceptualized in study one, and the development of an exploding foil device. This exploding foil device was tested by itself using copper foils coated with graphite powders. These discharges attempted to develop a conductive surface layer with good friction and wear properties by driving graphite into substrates with copper plasma. This overall group of experiments, exploding wires and exploding foils, was soon dropped when a new concept emerged. The new concept was to use the exploding devices in conjunction with a railgun. No longer would a significant loss in railgun energy be required. The railgun could be connected to one discharge bank or homopolar generater, and the plasma device to another.

The second study then ended with a group of experiments using an exploding wire device between the rails of a railgun. The deposits obtained in this configuration were characterized as either nil or very inconsistent. In fact, after a nine shot series, the total deposition was found to be only 40 nm thick. The error here

was not conceptual, but lies in the fact that not enough material was present between the rails to sustain such an energetic plasma arc.

This thesis therefore incorporates the use of a new exploding foil device to feed an open bore railgun. The overall purpose was to further explore the capability of a high energy railgun accelerator as a material deposition tool. The specific aim was to produce unique depositions, and possibly novel materials or coatings not readily attained by other means. Characterization of the produced depositions therefore became an important and necessary aspect of the research. Additionally, the scope was kept broad to hopefully expose this technique's advantages. Finally, to improve overall results, hardware improvements and modifications were made through the project.

CHAPTER 2

EXPERIMENTAL SETUP

The actual railgun system used for this research was housed at The Center for Electromechanics, University of Texas. It was operated jointly by CEM and The University of Texas, Center for Materials Science & Engineering, under NADC contract.

RAILGUN HARDWARE

Figure 3 is a simplified schematic of the experimental configuration. Basically, a high voltage power supply was used to charge two capacitance discharge banks rated at 9.6 and 25.0 kilojoules of energy respectively. These banks were attached to an open bore railgun, and an exploding foil device through very low inductance bus work and coaxial cables. Ignitron switches were used within the circuitry for timely triggering of the banks. These ignitron switches were rated at 350 kA and became one of the limiting factors of the equipment. Although not used in our experimentation, a quick pulse homopolar generator could also have been used as the energy source. If this were the case, storage inductors would be required within the circuitry. As shown, both the rail electrodes, and the exploding foil device were housed within a vacuum chamber. This chamber was typically evacuated to 1.5 x 10^{-4} Torr. The vacuum system included an oil roughing pump, and a cryogenic pump. Evacuation serves two purposes, first it prevents premature voltage breakdown as described by Paschen curves, (20) and secondly the deposition is

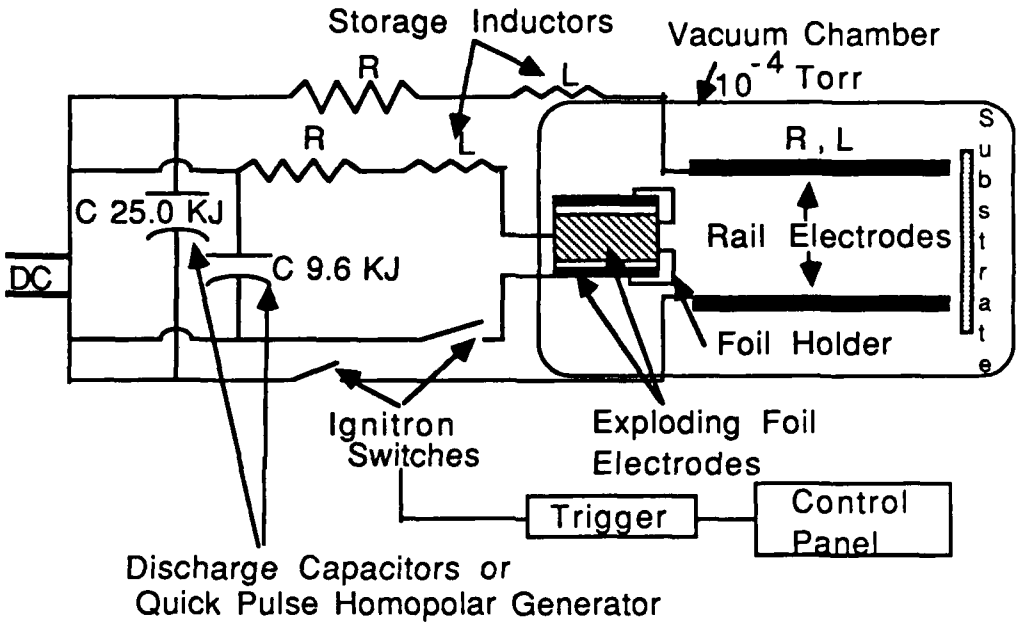

Figure 3 : Experimental Setup

somewhat cleaner. However, the ultimate vacuum in the system was significantly lower than required for clean deposition processes and will need upgrading. Finally, the chamber and rails were configured with various instrumentation probes and a substrate holding device. The specifics of some of the important components will now be discussed.

First, the railgun electrodes were of two different types in two distinct geometric configurations. Type one was square bore, height of each rail equal to the parallel spacing, width (See Figure 2 for convention). Two sets of this type were used. The first set measured 5 x 5 x 25 cm, and the second 5 x 5 x 35 cm. The other type of rails were trapezoidal in shape. The trapezoidal electrodes narrowed in both height and spacing along their length. These electrodes were designed and manufactured later in the project to successfully focus the plasma arc, and to change

the overall characteristics of the deposition system. This change will be discussed in detail in Chapter 4. One set was manufactured. These rails were approximately 50 cm long and tapered from 15 to 5 cm in height over their length. When mounted, the vertical bore spacing (width) also decreased progressively from 5 to 4.4 cm. See Appendix 2 for actual schematic. With regards to rail configuration, the electrodes were primarily aligned such that their long axis was parallel and coaxial with the main stream of exploding foil material. This is most logical and provides the highest possible arc velocity. It also provides the highest material deposition efficiency. The second configuration involved placing the rail electrodes long axis at 90 degrees to the material stream for filtering. This will also be discussed later.

The new exploding foil device was designed after Grevtsev's schematic (21), and is capable of generating a significant amount of plasma. It consists of two coaxial electrodes, one inside the other, and a foil holding cap. Current flowed through the outer electrode across the foil and back out the inside electrode. This created a current density build up within the foil and subsequent vaporization. These electrodes were separated by an alumina insulating sleeve to prevent arcing. The cap also contained a washer to insure positive contact between the foil and the electrodes. The blow out diameter of this cap was 2.5 cm, and foils were successfully tested to .28 mm thick. The inner electrode was approximately 7 cm long by 1.25 cm in diameter. It became a critical component during experimentation.

Now, in an attempt to better characterize the overall process, instrumentation was used. Rogowski coils served as current measuring devices for both the railgun and the exploding foil device. The corresponding voltages were obtained with resistive dividers. The experimental setup also included photo-transistors or B dot (rate of change of magnetic field) probes. (22) These

transistors and probes were placed along the length of the railgun. If oriented correctly, they yield a signal proportional to plasma light intensity or armature current. When plotted against a time scale on an oscilloscope, one can deduce the armature position, and therefore the arc velocity.(22) As these velocities were very fast, a scope resolution of 20 nsec / point was required. See Appendix 1 for actual hardware photographs.

MATERIAL SYSTEMS AND SETUP

As this research is in its infancy, several metallic material systems were investigated, Figure 4. This broadness allowed for the determination of how this process may contribute to the already numerous deposition and coatings methods. However, in most cases the specific material system was also selected with a purpose in mind. The only exceptions being, glass, polyimide, and single crystal NaCl substrates. The glass and NaCl substrates were selected for ease of post shot analytical examination. Kapton tape, polyimide, served as the visual comparison between all systems. It was also used as a means of attaching the substrate to the holding device, as it is a good vacuum reasonably high temperature material.

The starting deposition material was primarily in foil form. Normal foil thickness was between .013 mm and .076 mm with a 2.5 cm circular diameter. This yields an exploding material weight ranging from approximately 70 - 200 milligrams. Elemental foil purity was at least three nines. These foils were loaded within the exploding foil device as single charges, or back to back up to three thick. The latter yields more deposition mass, and the possibility of species mixing in the plasma , vapor, and liquid state, or metallic compound formation.. An example would be shot

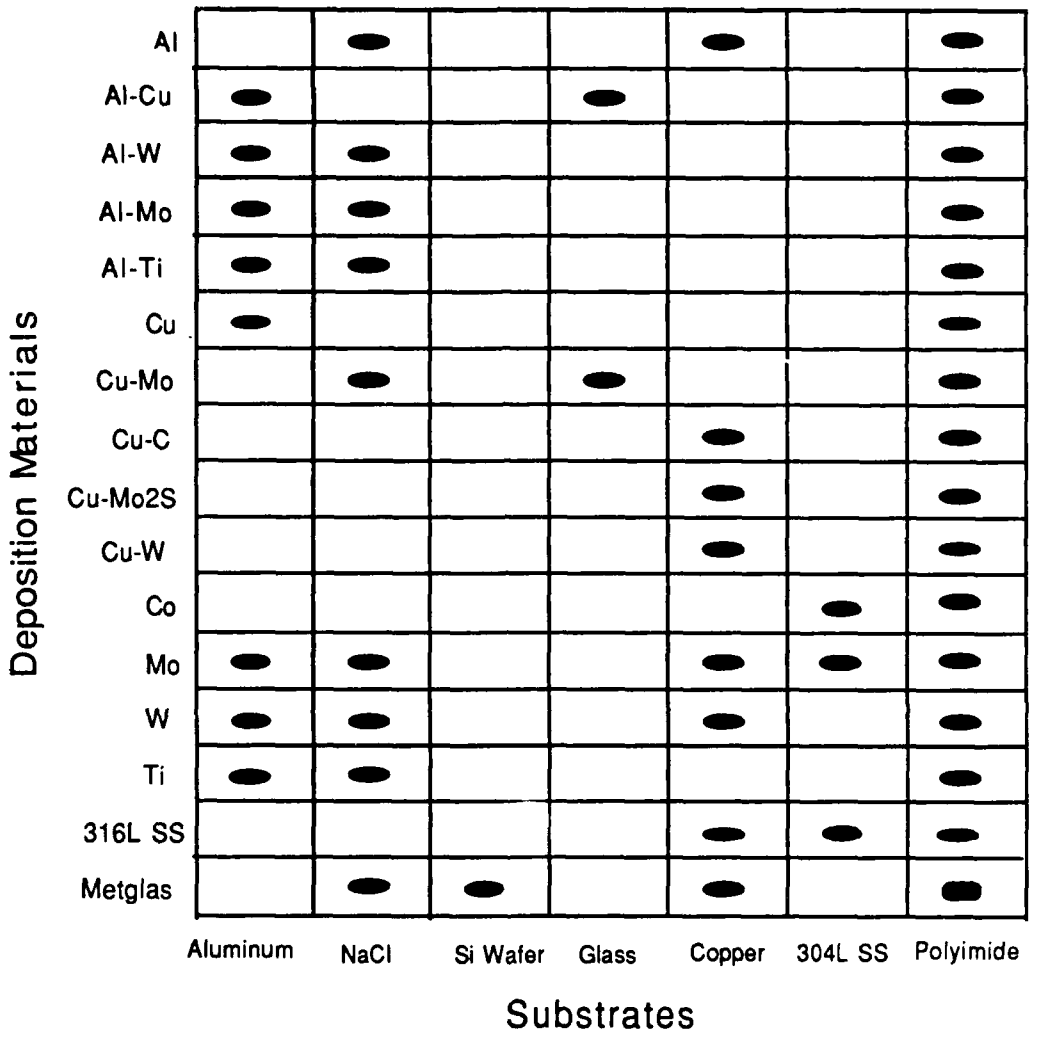

Figure 4 : Material Systems

76 where the charge was .025 mm Al, .025 mm Cu, .025 mm Al loaded back to back. In addition to multi - element foil shots, foil and powder packets were also tried. One such shot, # 120, involved a .025 mm copper foil packet filled with Mo_2S powders.

The metallic substrates, Al / Cu / 304 L SS, were generally .25 mm thick shim stock measuring 5 x 5 cm. A few experiments did however use substrates as thin as .025 mm and as thick as 1.25 cm. These substrates were normally placed 2.5 cm beyond the end of the rails. However , in an attempt to better understand the machine, some experiments involved substrates located along the sides of the rails, and between the rails. Specific to the 90 degree configuration, substrates were also placed directly across the rails in front of the exploding foil device. This placement of the substrates in various different positions yielded some interesting results to be covered in chapter 4.

In addition to placing the substrates at various locations, the amount of surface preparation was varied. This preparation ranged from raw material, no prep., to electropolishing or mechanically polishing and then solvent cleaning just prior to mounting and evacuation. Abrasive cleaning was also employed throughout the project. This system was not however set up to perform in vacuum sputtering prior to discharge. As it also took approximately 45 minutes to evacuate the camber to the 10^{-4} - 10^{-5} Torr range, clean here is only a matter of degree. But, the attempt to have an active surface was made.

CHAPTER 3

ANALYTICAL TOOLS

To better understand and attempt to quantify the capabilities of the railgun system as a deposition tool, the various metallic coatings and thin films produced were analytically characterized. As the breadth of characterization is so wide today, this study focused upon the microstructural aspects of the deposits and not upon the physical properties. With this emphasis in mind, four complimentary analytical tools were chosen. These were X-Ray Diffraction, Scanning Electron Microscopy, Transmission Electron Microscopy, and Auger Electron Spectroscopy. This chapter will briefly discuss the merits of these techniques, and how they were used for this research. An excellent reference is provided for in depth study.

X-Ray Diffraction (23)

Based upon the findings and theories of Laue, Ewald, and Bragg, present day X-Ray diffraction allows for the complete determination of material crystal structure. More specific to this research , one instrument, a diffractometer, irradiates a specimen and then scans and records the diffracted X-Ray signal over a selected angular (2 theta) range. The received pattern consists of a series of characteristic peaks with varying intensity that satisfy Bragg's law. As each phase is distinctly different, the spectra (peak position and associated intensity) becomes a fingerprint for material identification. The JCPDS (Joint Committee on Powder

Diffraction Standards) has compiled an index of spectra for more than 70,000 existing elements and compounds. One can match their unknown against these standards for identification.

X-Ray diffraction was then used as a tool for relative quick determination of elements, compounds, and or second phases present in the samples. By todays standards, it yields a bulk analysis. Depth of measurement is typically between 10 and 100 microns. In addition, the absence of discrete sharp peaks within a spectrum (one broad hump from diffuse scatter) is possibly an indication of non-crystallinity, the glassy state.

For this research, a Phillips powder diffractometer linked to an IBM Series I minicomputer was used. The X-Rays were Cu K α, wavelength 1.5405 Å. The X-Ray beam was monochromated in the post reflecting position by a graphite crystal. The specimens were rotated to reduce preferred orientation, and in most cases the two theta angle was scanned from 10 - 90 degrees. An IBM search-match routine or the Hanawalt method was used to determine the results.

SCANNING ELECTRON MICROSCOPY (24)

The scanning electron microscope (SEM) has the same basic purpose as any optical microscope, to render tiny objects visible to our eyes. There is one big difference, an SEM uses an electron beam as the probe source and not visible light. As such these microscopes are capable of achieving resolutions of less than 10 nm with an excellent depth of field. Also, once the electron beam strikes the material, it interacts very strongly to produce an electron - quantum yield .

This yield is then detected, amplified, magnified, and presented on a CRT screen. The end result is a high resolution "picture" of the sample in almost 3-D. Although visually like any other picture, this image is a subtle representation of the quantum effects of the beam.

Most SEM's are set up to detect secondary or backscattered electrons for image formation. As secondary electron image contrast comes from trajectory and number, an excellent topographic image is presented . Secondary electrons also yield superb contrast between conductors and insulators. Backscattered electrons on the other hand carry some number and trajectory contrast but primarily variation in density or atomic number, ideal for verification of second phases.

Although not directly used for image formation, the characteristic X-Ray yield is also important. An area can be imaged and then the emitted X-Rays analyzed by an energy dispersive spectrometer (*EDS*) for elemental analysis.

All in all, an SEM is a excellent analytical tool for microstructural imaging of a sample surface and subsequent chemistry information. The SEM work for this research was accomplished with a JEOL JSM 35C linked to a Kevex computer system. This computer analyzed and corrected the EDS signal for atomic number, absorption effects, and fluorescence effects. The resulting, presented, chemical analysis was accurate to approximately ± 5%.

TRANSMISSION ELECTRON MICROSCOPY (25)

Although somewhat similar to an SEM, the transmission electron microscope operates in a different manner. Due to its large potential, 100,000 V to 1MV, the electron beam goes through the sample and emerges as a transmitted

electron stream. The subtle differences of the transmitted bean, caused by the sample, are then used to develop image contrast. Because an electron has a finite elastic range within matter, a thinned specimen of less than approximately 200 nm thick is required. Also, as the beam is much more energetic for this process, the electron wavelength is shorter and resolution is greater. Lattice planes can actually be resolved at the 2 Å level. Normal point to point resolution is limited by the lens system but is still below 2.5 nm. Magnifications to and above 450,000X are not uncommon.

In addition to images of the tiny microstructure, one can also obtain electron diffraction patterns just like those found with X-Ray. Two types become available. For single crystals, spot patterns are generated which yield the crystallographic structure. For polycrystalline specimens, ring patterns are obtained. These are akin to the X-Ray diffractometer spectra. They can be indexed directly using the Hanawalt method against the JCPDS standards to determine the elements, second phases, and or compounds. Again a large diffuse ring points to limited crystallinity.

The TEM can also be configured in a scanning mode whereby the beam is rastered over a specific area of the sample. This instrument is know as a scanning transmission electron microscope (STEM). These microscopes usually have the added feature of an EDS detector for chemical analysis. As most EDS's are only effective down to Na, the STEM is also generally equipped with an electron energy loss spectrometer (EELS). EELS is capable of detecting the lighter elements like C and O. Although EELS is not a mapping tool it gives semi-quantitative numbers on the elements present within a selected area of the sample.

The micrographs, ring patterns, and EELS spectra presented in this research were obtained using a JEOL JEM 200CX TEM, and a JEOL JEM 1200 EX STEM.

The STEM was configured with EDS and EELS detection. A Tracor computer and data analysis system was also linked to the STEM.

AUGER ELECTRON SPECTROSCOPY (26)

The final analytical technique used was Auger Electron Spectroscopy (AES). As most of the useful AES electrons emerge or escape from the top 2 nm of the sample, AES is truly a surface science tool. It is capable of detecting all elements above Li.

The Auger electron transition energies and associated spectra for each pure element are compiled into an Auger Handbook (27). Cross reference of an unknown spectrum against the handbook standards makes elemental analysis fairly straight forward. The relative sensitivity of each element's Auger yield is also compiled and therefore semi-quantitative analysis is possible. Even without the use of internal standards, the technique gives ± 10 % numbers. It is also capable of elemental detection to approximately 1% in solution.

Perhaps one of the most versatile ways of using this technique is in conjunction with ion sputtering. Although the sample is damaged by the sputtering process, one obtains an elemental map normal to the sample surface. This is commonly referred to as depth profiling.

The Auger spectra presented in this thesis were obtained using a Physical Electronics 590 instrument. Depth profiling was accomplished with high purity Argon gas. The presented depth profile plot was from a linked X-Y recorder; however, the associated atomic % plot was calculated from a continuous line recorder chart.

CHAPTER 4

RESULTS AND DISCUSSION

The results and discussion presented in this chapter are the findings of this researcher based upon 11 months of experimentation from April 1986 through February 1987. All total more than 150 discharges of the railgun system were accomplished. Although the specifics of each shot are not detailed, the knowledge gained from their uniqueness is incorporated into the overall text. Again the purpose was to attempt to define the possible working range of this railgun system, and to both qualitatively and quantitatively characterize the produced coatings and films. This material is also presented in a fairly chronological order so the reader can better understand the system development and knowledge progression.

COATING EXPERIMENTS

This portion of the chapter will emphasize those experiments which in general yielded the thickest depositions. These depositions are most comparative to the other bulk surface coating techniques like plasma spraying. The samples were obtained with the railgun and exploding foil device in their original and most logical coaxial configuration.

The first series of experiments involved five discharges. These original discharges were merely aimed at testing the machine , and setting up the instrumentation parameters. The shots involved vaporization of .025 mm Al foils and subsequent railgun deposition on .2 mm solvent cleaned copper targets. The stored

bank energies were 9.2 kJ for the EFD and 3.4 kJ for the railgun. It was immediately apparent that the new exploding foil device had fulfilled its purpose by generating a significant amount of plasma, vapor, and liquid deposition species. A fairly uniform deposit was obtained across the entire target area of 25 cm^2. From SEM analysis, the depositions were found to be approximately 20 microns thick and surface coverage was estimated at 85%. Based on these findings and weight measurements, the overall material efficiency was roughly 35%. However, being an open bore apparatus, the machine was not specifically designed for efficiency. In fact throughout all coating experiments, the material efficiency remained between 20 - 40 %. It was interesting to find that Yushkov (28) predicts an efficiency between 10 and 50 % using his mathematical model for the behavior of plasma jets and thermally produced particles.

Next, the surface of these depositions was characterized as being fairly rough in texture, both visually and under the microscope. It appears that the last material down is either liquid in the form of droplets or as a result of inadequate wetting, material spheres on the surface, Figure 5. As seen, the particle spheres are sized at 15 microns and smaller. There is also evidence of a splatting effect on the surface. The material splats range from approximately 50 μm down. The presence of these spherical particles and surface splatting has been reported by other investigators of pulsed plasma deposition. (17, 18, 29, 30, 31) In fact, with the exception of one group, to be discussed latter, the elimination of these surface particles has been elusive. Finally, adhesion of the coating to the substrate was found to be very poor. The coating was easily pealed off.

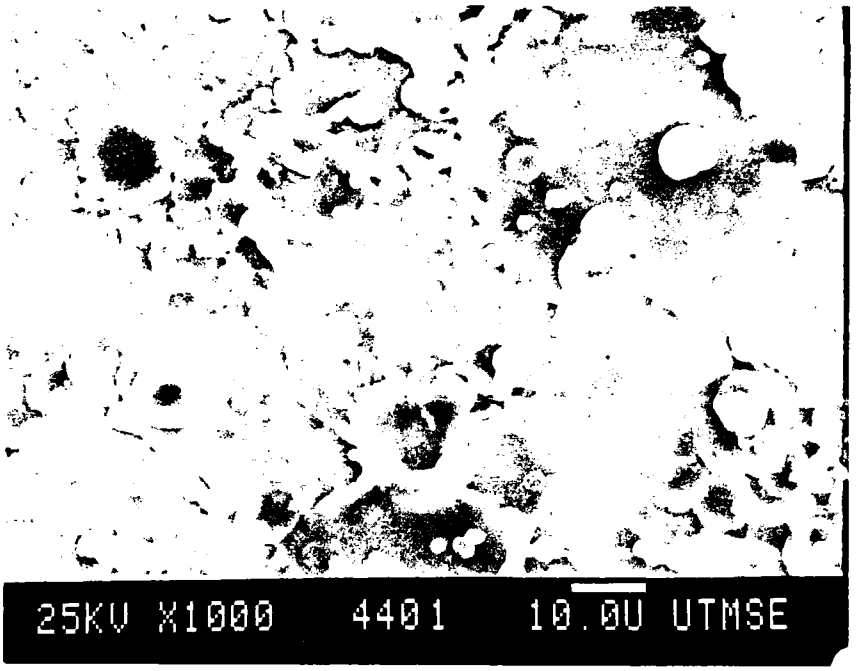

Figure 5: SEM Micrograph of an Initial Deposition Surface

The second series of experiments was aimed at increasing surface coverage. Two .025 mm Al foils were loaded back to back in the EFD and the energy was raised to 12.5 and 4.7 kJ. Nearly 100 % surface coverage was obtained on the copper targets.

The following series of experiments, reversed the element roles. Rolled copper foil (.075 mm) was used as the deposition species, and the targets changed to solvent cleaned .2 mm aluminum. Surface coverage was excellent, and the texture remained the same. Despite the increased foil thickness with no energy increase, it was surprising that a noticeable improvement in adhesion was obtained. Some rubbing effort was required to remove the deposit. Also at this early stage in the research (shot # 12) , the EFD center electrode (aluminum) had begun to erode, and

needed replacement very soon hereafter. Electrical erosion of material components, in particular the rails, will play a role from here on out. Thereby those interested in high energy pulse power research should take heed of this effect from the start, and not have to learn as we did. Our improvement efforts in this area are detailed latter in the chapter.

To further investigate the relation of either melting or vaporization temperature and surface adhesion the next shot was .025 mm Mo at both copper and aluminum substrates. The deposition was rubbed off the copper with effort but was very tenacious on the aluminum. It was therefore concluded at this point that the difference in either melting or vaporization temperature of the couple plays a large role in adhesion.

Although one would reasonably place a target at the end of any gun type set up, the next series of experiments (8 total) looked at other configurations. These experiments also used a new material system 316L SS at aluminum targets. In this series the targets were initially placed outside the rails along its length. That is, they were parallel to the side of the plasma stream not perpendicular as before. The deposition would be a sweeping type effect across the face of the target. As seen in Figure 6, the surface morphology was much different than before. As expected, it looks like the plasma has run across the surface. These targets also had qualitatively good overall adhesion. The second target configuration involved placing a group of targets, 2 or 3, between the rails to effect a screening process. These targets were placed perpendicular, in the way of the plasma flow. There back to back spacing was 5 cm. A final target, in its normal configuration 2.5 cm beyond the rails end, was also used. It was found that each target had a deposit. In addition to a thinner as you go effect, the surface texture (particle size) was also progressively finer with each

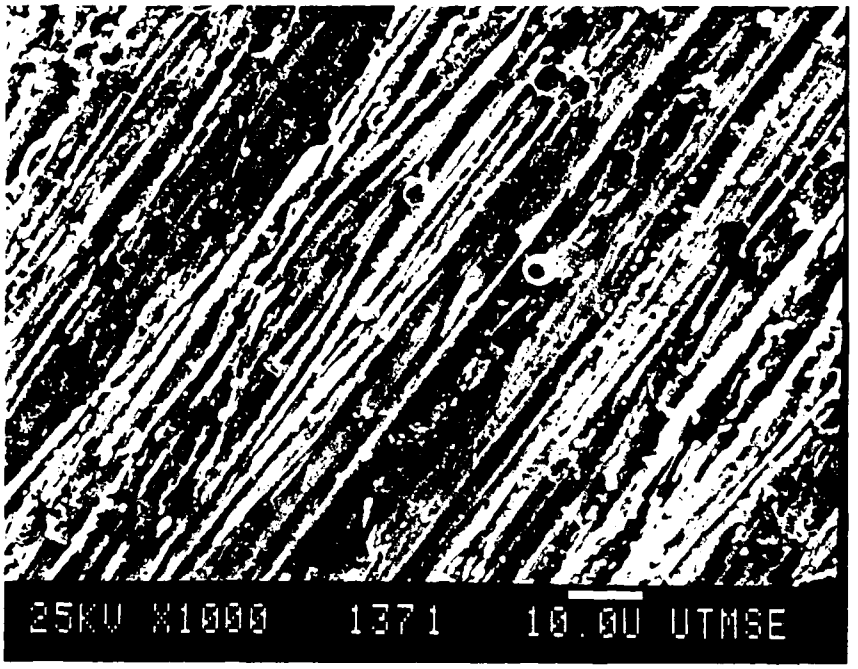

Figure 6: SEM Micrograph of a Parallel Placed Target -Distinct Morphology Change. Plasma direction coincident with directionality of micrograph.

succeeding target. A screening process had in fact taken place. This led to the conclusion that the lighter portions of the plasma arc, presumable the vapor phase ions and very small liquid droplets, could be moved around or directed by the energetic rails.

Next, to somewhat establish the upper limits of the deposition system, foil thickness was progressively increased to .28 mm of copper. A nichrome mesh of .94 mm wire was also attempted. The EFD successfully exploded about 50% of the .28 mm copper foil and a large portion of the .94 mm nichrome wire mesh. Adhesion to the substrate in these experiments was very poor. This might be expected as no doubt the plasma velocity, presumable lower here, plays a part in the

adhesion process. As the deposits easily peeled off the substrates, both the cross section and the first material down or bottom could be investigated. Deposit thicknesses were between 100 and 200 microns. Each deposit also showed a spread in its own thickness of about ± 25 microns. This yielded a fairly rough surface. Porosity was also evident from the cross section view. With regards to the bottom of the deposit, as shown in Figure 7, it was interesting to find that seemingly little vapor phase was present during these depositions or no surface wetting occurred. Even the back side or bottom showed the appearance of liquid type droplets. Although not investigated in this research, the micrograph leaves one with the idea that producing powders for metallurgy is a possibility.

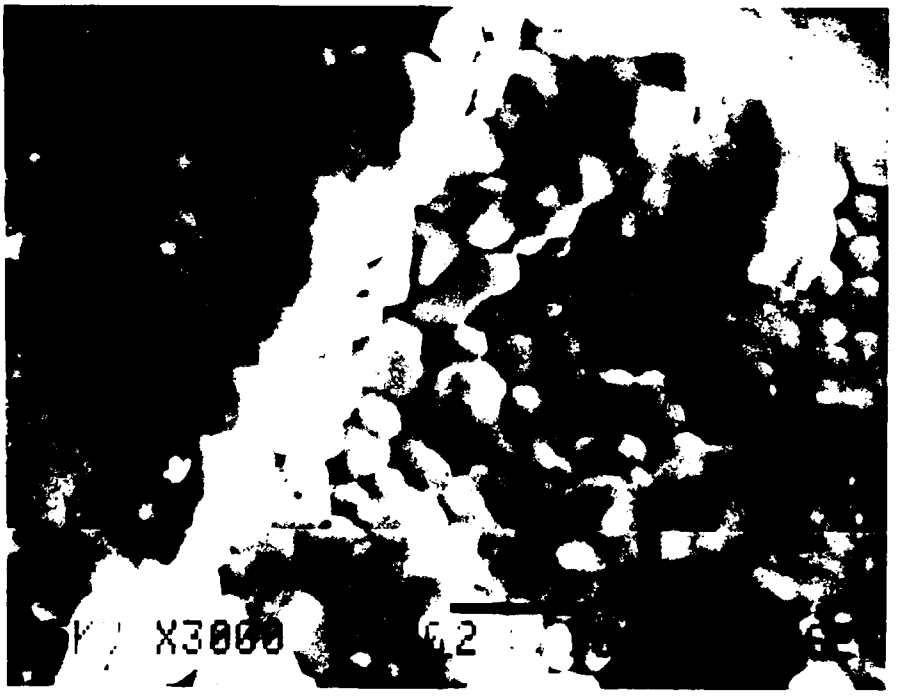

Figure 7: SEM Micrograph of Thick Deposit, View From Back Side.

To now determine the energetic nature of the plasma arc a series of three shots involved using .05 mm copper fuses at thin .025 mm aluminum targets. The dissipated energy still remained 12. 5 and 4.7 kJ respectively. Upon opening the vacuum chamber after the first shot, it was found that the .025 mm Al target was completely vaporized. On shot two, by using one screening target, 50 % of the final target survived, and subsequently on shot three , using two screens, 100% survived. However, even target number three displayed a large amount of surface melting. The observation of surface melting and a subsequent resolidified coating has been reported by others working with high specific energy condensing plasmas. (32) From X- Ray diffraction of the third discharge, shot # 72, it was found that in addition to the pure elements Al & Cu , the intermetallic compound of $CuAl_2$ (JCPDS Card 25-12) had been formed. See diffraction pattern Figure 8 and indexing Figure 9. This result lead directly to the next area of research, termed plasma mixing.

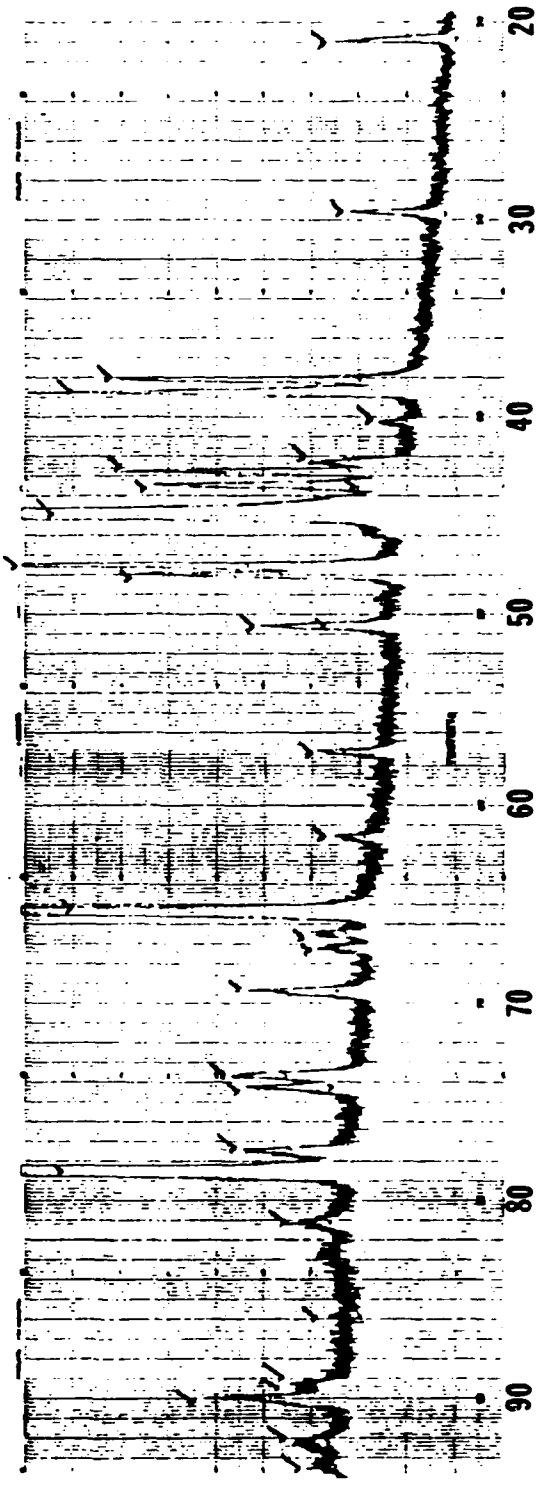

Figure 8 : X-Ray Diffraction Pattern of Shot # 72.

2 THETA ANGLE	D SPACING	Al 4 - 787	Cu 4 - 836	$CuAl_2$ 25 - 12
20.90	4.25			(110)
29.60	3.02			(200)
38.10	2.36			(211)
38.77	2.32	(111)		
42.35	2.14			(220)
42.80	2.11			(112)
43.43	2.08		(111)	
44.80	2.02	(200)		
47.50	1.91			(310)
48.00	1.895			(202)
50.55	1.804		(200)	
57.30	1.607			(222)
61.60	1.506			(312)
65.20	1.428	(220)		
66.50	1.406			(411)
67.30	1.392			(213)
69.40	1.355			(420)
73.70	1.286			(402)
74.21	1.277		(220)	
77.50	1.230			(332)
78.40	1.218	(311)		
81.10	1.185			(422)
82.60	1.164	(222)		
85.90	1.131			(204)
89.30	1.097			(521)
89.30	1.094			(413)
89.95	1.089		(311)	
92.25	1.069			(512)
93.50	1.058			(224)

Figure 9: Index of Preceding X-Ray Pattern (Shot # 72), Figure shows indexed hkl planes for the three materials, based upon the corresponding 2 theta angle and d spacing.

PLASMA MIXING

To pursue the possibility of further compound formation, a new idea was attempted. Instead of the mixing of elements on the substrate by diffusion or a melting process as previously described, both elements were now vaporized simultaneously within the EFD. This latter technique might allow for the mixing of species in the plasma , vapor, or liquid state. These experiments were accomplished by simply loading the different elemental foils back to back within the EFD. A sample charge might be .025 mm Al, .025 mm Mo, .025 mm Al. The rails were still configured coaxially with the targets placed 2.5 cm beyond their end.

The first system investigated was Cu and Al. The starting fuses were in a 50 - 50 atomic percent couple. The substrates used for these shots were aluminum and glass mounted side by side. Glass was chosen as the additional substrate for ease of X-Ray diffraction analysis, and also as a comparison where a plasma - substrate mixing interaction involving compound formation was precluded. The first few discharges were unsuccessful as the glass substrates fractured into thousands of pieces. These experiments did however give the indication that the force behind the railgun arc is quite large when compared with other deposition techniques. Subsequently a shock absorber device was constructed to eliminate glass fracture.

Overall, the results of this series were hard to quantify yet seemingly successful. First, weather on the aluminum or the glass substrate the same compound formation took place. In addition to the primary elements, the indexed patterns again showed the presence of $Cu\,Al_2$. But now the additional compound Al_4Cu_9 (Figure 10) had also been formed. Second, by merely changing the order

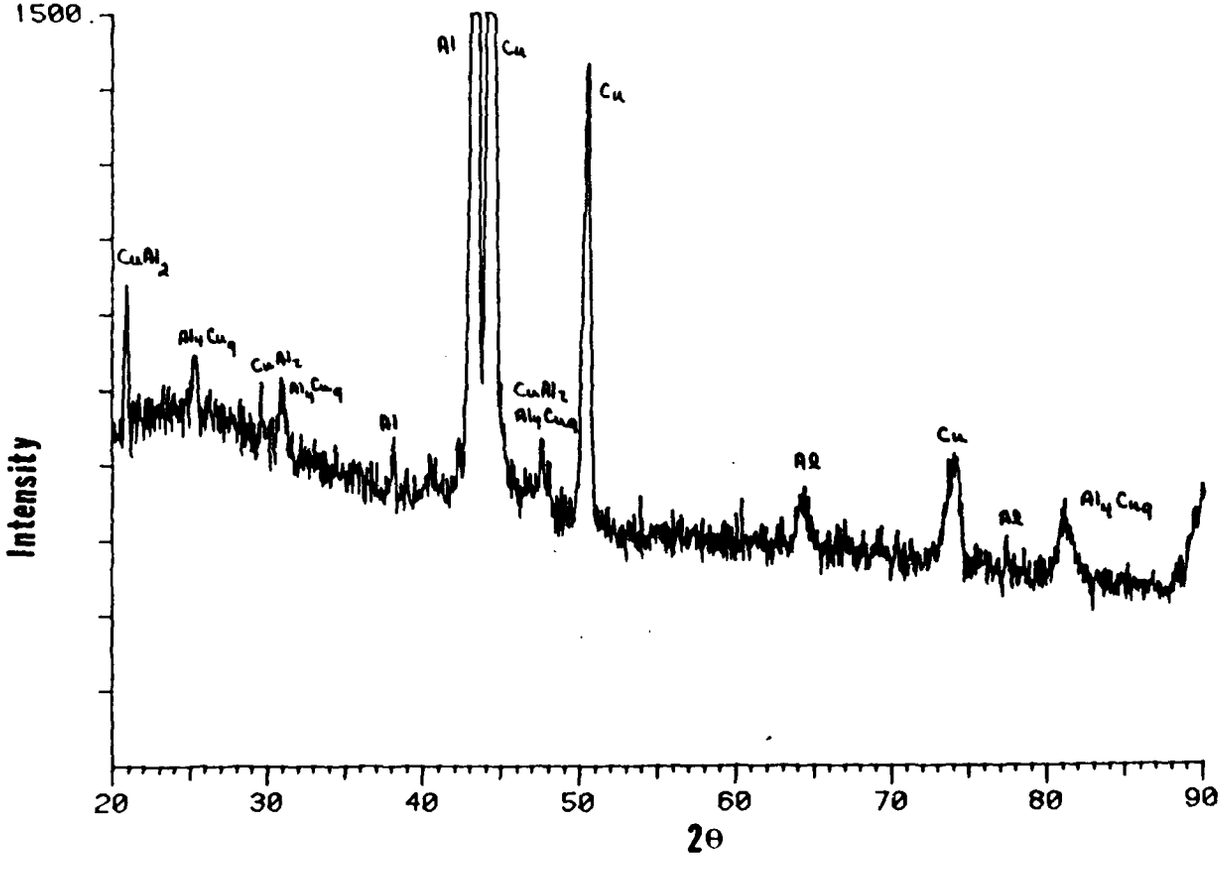

Figure 10: X-Ray Diffraction Pattern of Shot # 79, Pattern shows the additional phase Al 4 Cu 9.

of the fuses, the Cu Al_2 phase could be changed to $AlCu_3$. Although not totally conclusive, these results do indicate that plasma mixing is possible. However, compound formation could still be a result of the substrate quenching effects. That is, a third selected substrate with unlike thermal conduction may yield completely different results. This hypothesis was not tested. Simply, for these two substrates, the results were consistent. Also as the starting atomic percentages played no apparent role, presumably the most stable phases had formed.

Now, as the production of metastable phases by pulse plasma crystallization has been previously reported, (33, 34) the next set of experiments were aimed at producing a compound between the materials Cu and W or Cu and Mo. A couple between these materials might have possibilities as a surface coating for use in projectile railguns, that is a good wear surface with high electrical conduction. By conventional methods, these immiscible materials are even very hard to mix, and therefore only produced in small amounts or sections by infiltration techniques. This is because at the normally attainable elevated temperatures they are not in like states. As an example, when Mo is a liquid, Cu is a gas.

By plasma mixing it seemed possible that a quenched in structure from the gas and liquid state might be produced. The set up involved dual elemental foils in the EFD and .2 mm Cu targets.

The series of experiments yielded no indication of compound formation between these elements. X-Ray analysis showed pure Cu and Mo or pure Cu and W. However from SEM studies, the materials were mixed very evenly together. This in itself might be useful to produce a fine structure immiscible material plasma coating. Also, despite the lack of compound formation, adhesion to the substrate was found to be very good. The coating could not be rubbed or scraped off. This positive result

was probably attained due to either substrate melting and subsequent resolidification (3) , or possibly the plasma copper helped match across the interface. Examination of a thinned region of one of these shots in the STEM also yielded an interesting and expected observation. Using both the scanning and transmission mode, one was able to clearly see that the deposition was graded. The top remained a conglomeration of spherical droplets, but as one scanned downward towards the deposit - substrate interface, the scale became finer and finer. The first material down clearly appeared to be a vapor deposition. Figure 11 shows this microcrystalline region of the sample. Thereby, the lighter portions of the arc were experiencing a greater acceleration.

Faced with the limited success of the previous series, the most recent mixing experiments involved the coupling of aluminum with the refractory metals, Ti, Mo, and W. These experiments were designed to produce some of the existing aluminide phases. Those which have the unique property that fracture toughness remains high at elevated temperature. The atomic percentage of aluminum was varied from 33 to 66 % within each couple. The stored discharge energy was also raised to 20.6 and 8.7 kJ for the EFD and railgun. This was accomplished to enhance the vaporization of the refractory metals. Additionally, to supply more energy in a shorter period of time, the overall system inductance was lowered by modifying the current carrying buswork.

Despite the more careful control with this group of 15 discharges, the primary goal remained elusive. No intermetallic compounds were formed between the starting fuse elements. What did occur was that the couples reacted and formed oxides. Figure 12 is an example of one of the discharge X-Ray patterns where tungsten seemingly pulled oxygen from within the vacuum chamber and formed W_3O in addition to the pure elements. The other systems produced various Al oxides, Ti

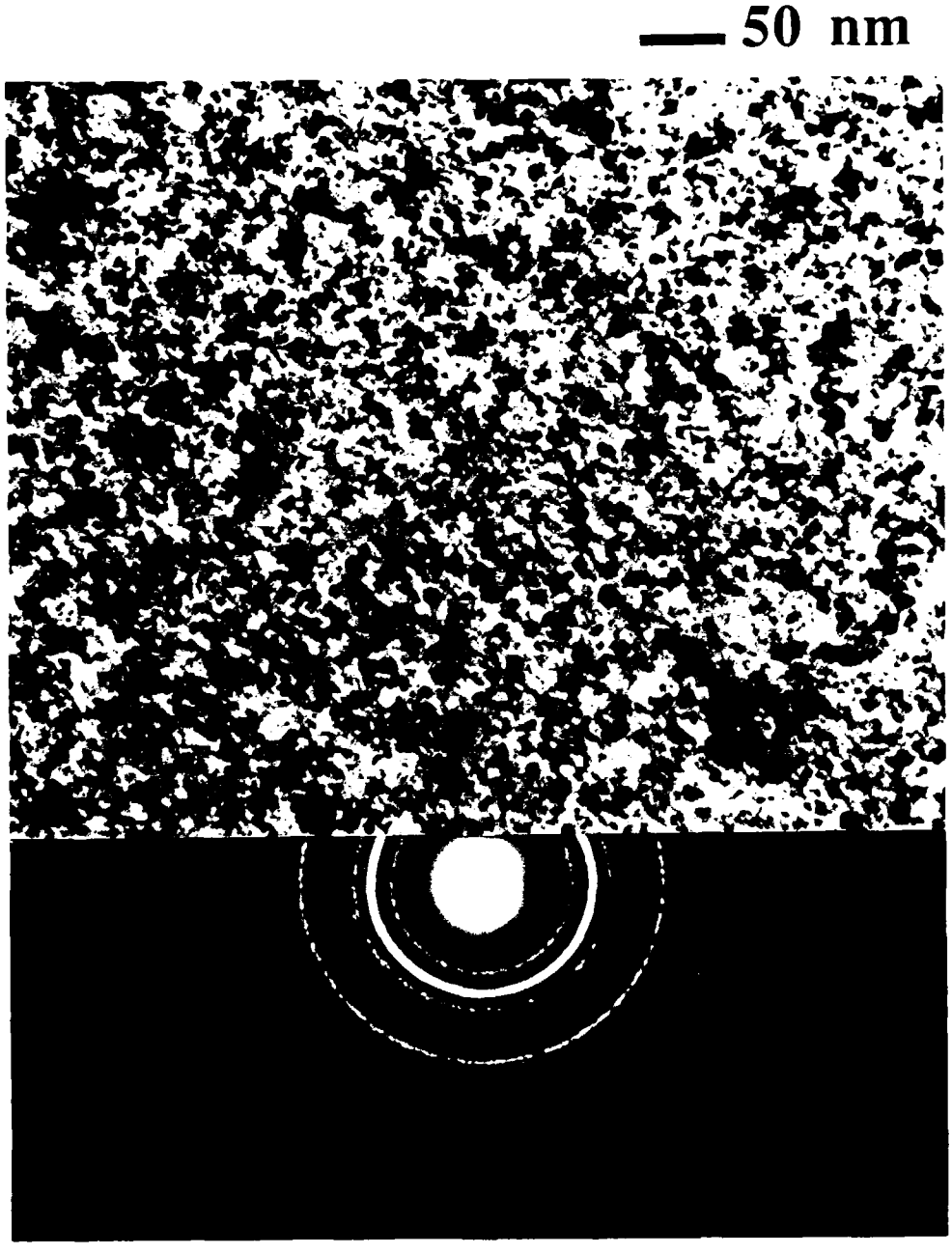

Figure 11: STEM Micrograph and Associated SAD Ring Pattern of Shot # 92 . Micrograph and SAD indicate a microcrystalline mixture of Cu and Mo.

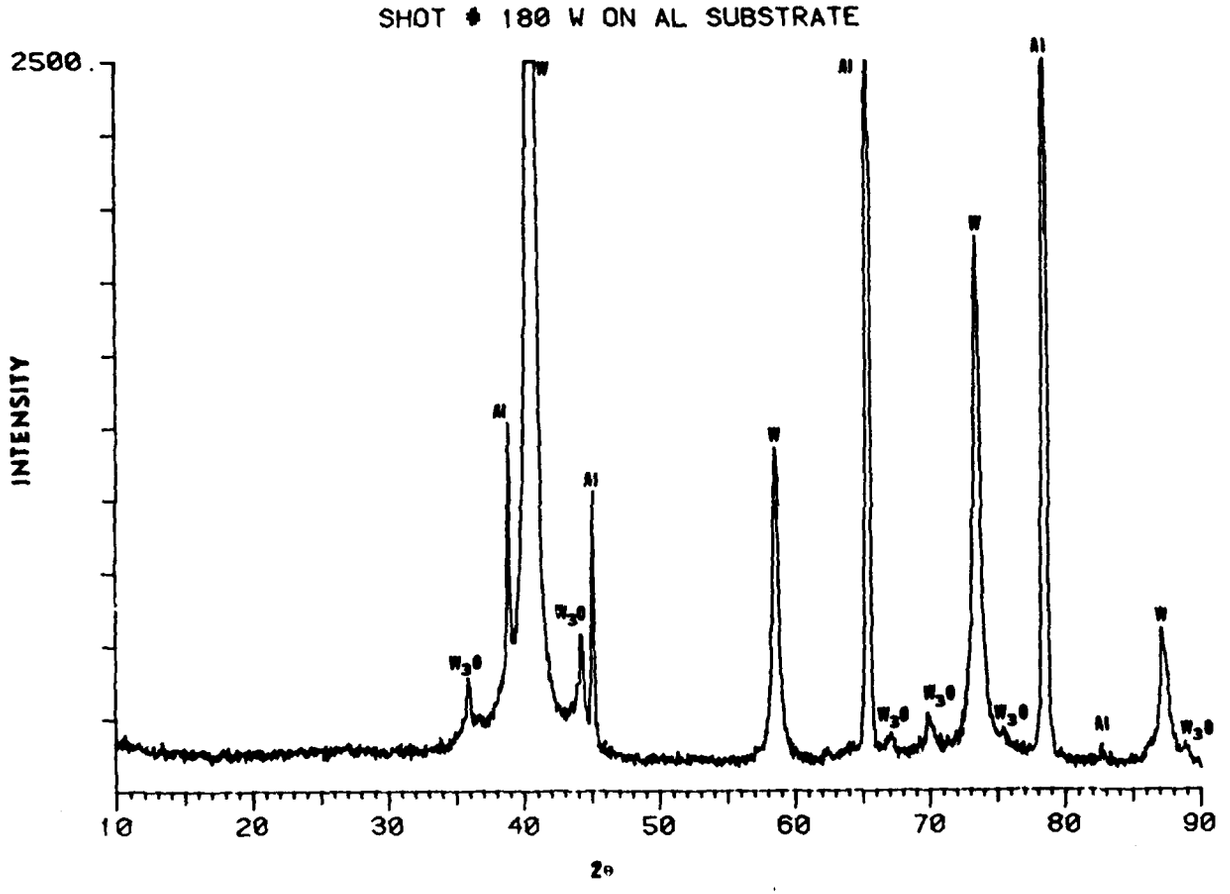

Figure 12: X-Ray Diffraction Pattern of Shot # 180, Pattern indicates the additional second phase W 3 O (JCPDS # 2 - 1138)

oxides, and Mo oxides with their associated pure elements. The tungsten and aluminum system overall was the most consistent. It yielded the above phase for each shot despite starting atomic percentage differences. SEM analysis of the group did however indicate that the materials were deposited very close to the starting atomic percentages, and that this was not the problem. It also showed that a uniform distribution of the elements had been attained across the substrate. It was therefore concluded that the oxides had formed due to the excess oxygen in the closest regions of the vacuum chamber and their lower free energy of formation (higher driving force). (35) A positive note for this series was surface adhesion. In all cases it was very good. Once again this pointed to an energy effect, and possible lattice matching across the interface. Also as seen in Figure 13, apparently due to this higher energy level, the liquid droplets were now much smaller than before, and no evidence of the splatting effect was found across the surface.

Although the plasma mixing experiments only showed promise within the Cu and Al system, it is still the contention of this researcher that the overall concept is good. First for the Cu and W or Mo couples, metastable quenching is not that likely, and second the set of Al and the refractory metal experiments really displayed a system problem. The arc was affected by chamber contamination. A high vacuum system backfilled or cleaned with a dry noble gas like Ar may make all the difference.

Also before leaving the plasma mixing section, it should be stated that in addition to multi-element foil shots, foil and powder packets were tried with success. One such shot, #120, was a packet of copper foil filled with Mo_2S powders at an alumina polished Cu substrate. The purpose was to investigate the friction and wear properties of the surface. Other packets of copper and graphite were also fired with

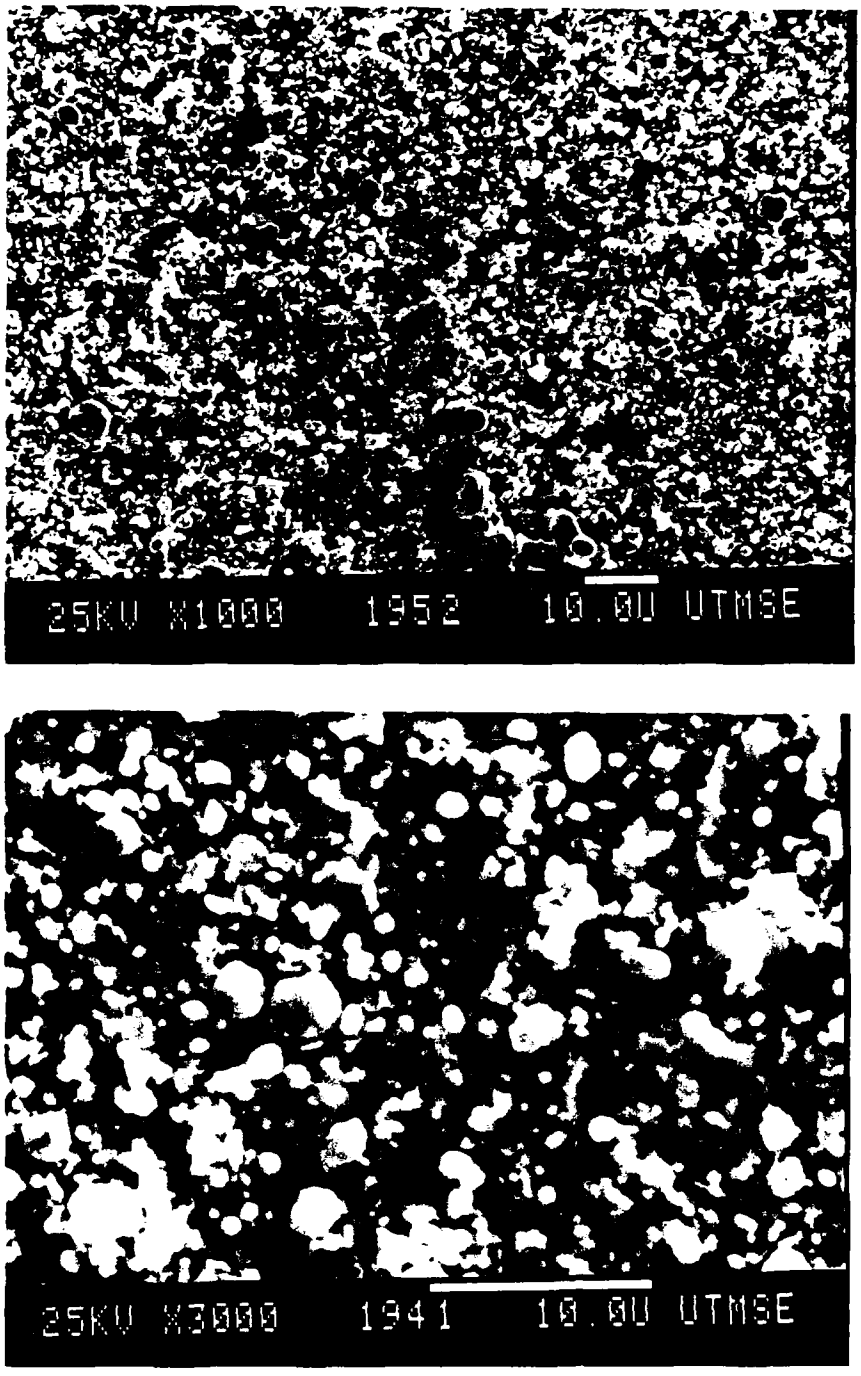

Figure 13: SEM Micrographs of Shot # 195 Co-deposited Al and Mo, Notice the much smaller liquid droplet size (≈ 5 μm down) and lack of surface splatting effect. a) Low Mag., b) High Mag.

success. In both cases the powders were carried along within the plasma stream and deposited by a drag type mechanism. This aspect of the overall research is being further investigated in detail by Chris Lund, and will be reported in his Masters thesis.

ADHESION

In a effort to further qualitatively determine the adhesion aspects of this coating process a series of approximately 10 discharges was planned and conducted.

The first set involved the firing of .025 mm Al at Cu substrates with the higher energy level of 20.6 and 8.6 kJ. Neither of the deposits showed good adhesion. It was concluded that the system as configured with its energy capability is not performing like an implanter type machine. That is, the eV of the ions is not high enough.

The next group entailed firing Cu at Al substrates prepared with varying degrees of surface cleaning, that is raw material, solvent cleaned material, polished material, and finally abrasively cleaned material. By far the best result was obtained with the abrasively cleaned substrate. Presumably the increased surface area and its active nature after abrasive cleaning made a big difference.

Now that it was determined abrasive cleaning produces the best results for this process, the stored energy level was consecutively ramped up from 9.2 and 3.4 kJ to 25.0 and 9.6 kJ. The fuse material was .05 mm Mo and the targets were abrasively and solvent cleaned .2 mm Al. With the exception of the lowest energy level deposition all coatings were soundly attached to the substrate and could not be scraped off. With afterthought, perhaps a less extreme couple should have been

chosen and the substrates just solvent cleaned; but, the one noteworthy difference makes the point. that energy enhances surface adhesion for this system. This increased adhesion stems from surface melting, material inter-mixing, and resolidification of the couple. Figure 14 shows the highest energy shot where the surface morphology has completely changed to show this aspect. Similar high energy discharges of W at Cu produced like results. It was also noted that a fair amount of substrate bending and deformation had taken place. Once again indicating the force of this deposition process.

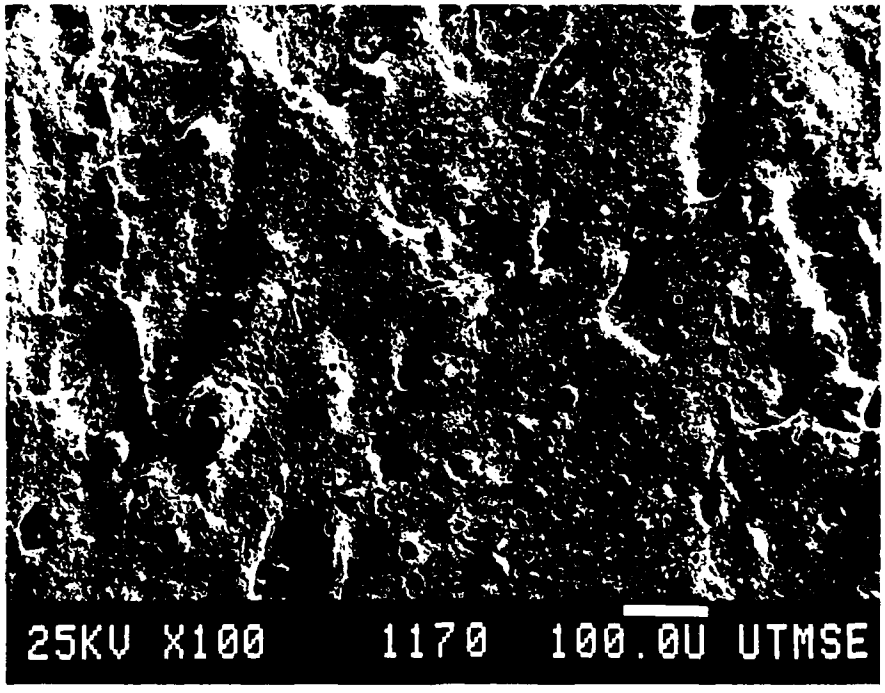

Figure 14: SEM Micrograph of Shot # 117 - Mo at Al Substrate, Highest energy level used, 25.0 kJ for the exploding foil device and 9.6 kJ for the railgun. Evidence of surface melting and resolidification.

Although not specifically designed within this group of adhesion experiments, some of the latter sets involved substrates from .64 to 1.27 cm's thick. Surface melting was noticeably decreased on these substrates, but the coatings were still firmly bounded. Perhaps just local interface melting and mixing occurred, followed by a self quench. Overall then, surface adhesion is best attained for this system by using a high energy level, material couples which have very different melting or vaporization temperatures (substrate being the lower), and substrate abrasive and solvent cleaning just prior to vacuum loading.

While pursuing the final effect of high energy input on surface adhesion, a system deficiency previously mentioned came to a head. Electrical erosion of current carrying elements within the system yields contamination of the deposit. Others have also seen the same effect. (31,36, 37) Figure 15 is an example of how

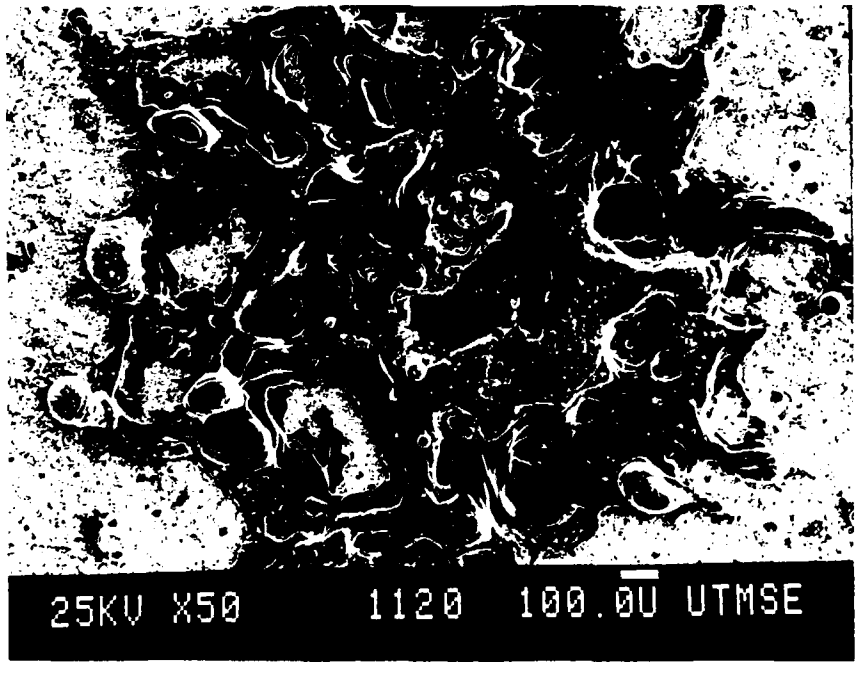

Figure 15 : SEM Micrograph of EFD Cu Contamination on Substrate Surface Shot # 112.

bad the contamination can get. The micrograph shows a large copper droplet on the deposition surface. From examination of the system, this copper droplet was determined to be an extruded portion of the EFD inner electrode. As system contamination became a real problem with this section of higher energy adhesion experiments, the research chronological order will be interrupted here to present all findings pertaining to this problem.

CONTAMINATION PROBLEMS

As previously indicated, very early in this research project deposition contamination by electrical erosion was noted. In fact the first observation was visual. Silver colored droplets were seen on the surface of a copper deposit. These droplets were presumed to be aluminum from the inner EFD electrode as all other current carrying components were copper. This was subsequently confirmed by EDS in the SEM. By shot # 20 it was deemed that this electrode needed replacement. The electrodes original shape was cylindrical with one end flat and the other treaded. The flat end which makes contact with the exploding foils had completely rounded by this point. That is, the end was now a hemisphere. This change in shape leads to current build up at the end's center and extrusion of material into the plasma stream. A second aluminum electrode was manufactured and installed. Again by shot # 40, the same process had taken place and replacement was necessary.

Owing to the fact that a large number of shots still remained, copper was attempted as an alternate material in the hopes that it would behave better. Once again after approximately 20 shots extrusion began to take place. At this point, a literature search was accomplished for answers.

From Warne (38) it was found that the geometry of our cylindrical electrode causes approximately a 3.0 current density increase at the end edges. This would account for the change in shape to a hemisphere over time. However, this by no means solves the problem. As we found, once the electrode eroded to the hemisphere shape, in its effort to reduce the current raiser, it now had such a small contact area to the foils that the problem became much worse. The idea of a change in geometry was dropped.

Another aspect which enhanced the problem for our experimental set up was found to be the current skin effect. (39) Because of the lack of time involved, the current or pulse from a high energy short duration (< 10 micro-second scale) power supply runs right along the surface of the conducting elements. Current diffusion into the bulk of the material does not take place. The current only flows in the outward 50 - 100 microns. This effect has been shown to cause surface erosion through thermal fatigue, surface melting, and even surface vaporization. (39, 40) Now, given that we did not want a major component design change, and that the current skin effect could not be eliminated but would only intensify as pulse duration was shortened and energy increased (41), the only solution seemed to be a change in material.

Two excellent studies (41, 42) were found which dealt directly with the problem of electrical erosion and candidate materials. The best candidate material was graphite; however due to its high resistivity, graphite was not selected for our use. The second best material presented was pure tungsten. As machining of tungsten is a very difficult process, the new electrode was manufactured with approximately a 3 mm tungsten tip brazed to a normal copper cylinder. This electrode failed at the braze interface on the first discharge. The braze joint showed very poor wetting of

the surfaces, and the tungsten tip itself also brittlely fractured after separation. The choice then became either manufacture a solid tungsten electrode or go to a third material. Owing to its machinability, the third material was selected. This material is a new grade of copper infiltrated tungsten developed specifically for spark erosion. It is termed Plansee K33S or Elkonite. The chemical composition is 67% W, 33% Cu. This electrode was manufactured by the Scharzkopf Corporation. For all practical purposes, this electrode solved the EFD contamination problem. Even after using maximum power, the presence of liquid contamination droplets on the surface had stopped. Figure 16 is a comparative photograph of a pure copper electrode, and the new Plansee electrode after twenty discharges each. As one can see there is quite a difference in how the two materials behave. The copper electrode is basically

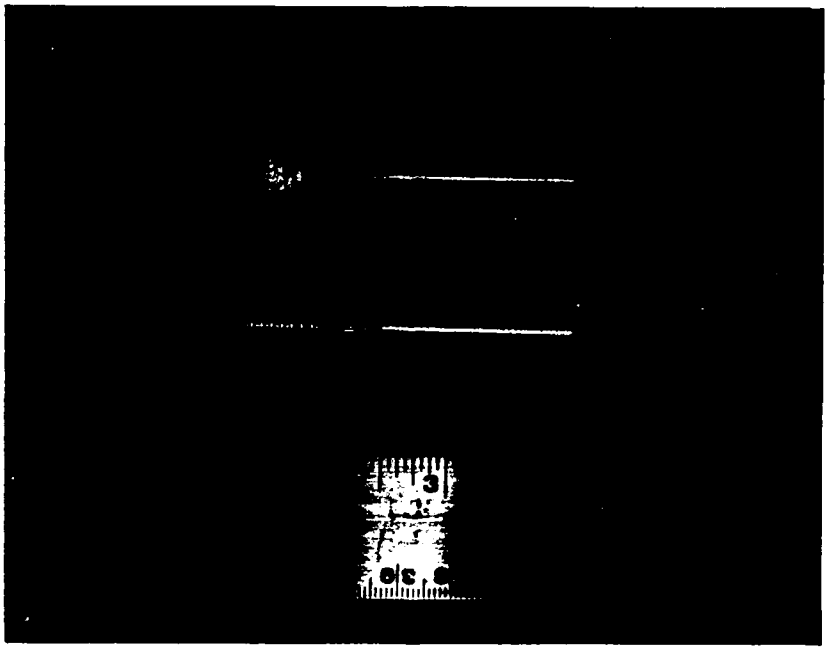

Figure 16: Photo of EFD Inner Electrode, Cu top, 67% W 33% Cu bottom.

finished and the new Plansee electrode shows little wear. As will be seen later, the inner EFD electrode was not the total contamination problem; but for this system, it was by far the weakest link and solving this problem was a major breakthrough. But before going on to a new contamination area, a short study will be covered.

As no material is perfect, towards the end of this research project, a comparative study between the erosion rates of the Al, Cu, and the new W-Cu electrode was accomplished. This study was aimed at further quantifying the difference between the three primary inner EFD electrodes. A pure Mo electrode was also manufactured and used as a fourth comparison within this study. The study involved discharging the electrode several times with pre and post shot weighing. Figure 17 is a graphic representation of the results on a weight basis.

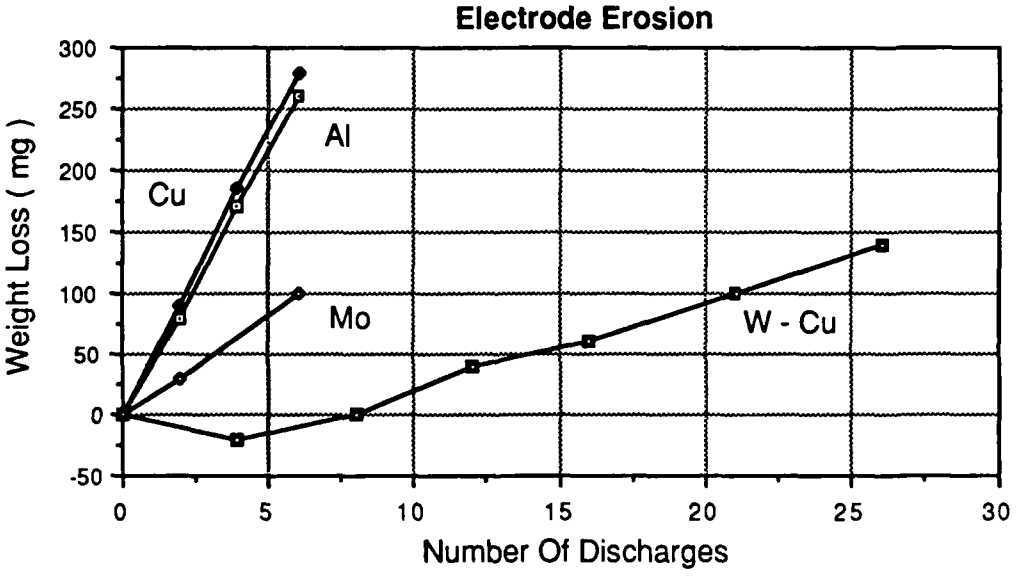

Figure 17: Erosion of Inner Exploding Foil Device Electrode.

Although a more precise study would involve volume loss per discharge, this graph still shows that in spite of being the heaviest material, the Plansee W-Cu electrode was eroding at a much much slower rate. Approximately a 5 mg loss per discharge versus 45 mg for the Al and Cu. When the weight difference is taken into account the Plansee wear rate is over an order of magnitude better. In fact, by the end of this research, the W-Cu electrode had been used for more than 40 discharges and it was just beginning to show evidence of visual erosion, rounding of edge ends. It was not however anywhere close to developing the previously found hemispherical shape. For our purposes, it was the preferable material. It could withstand the high current levels of approximately 350 kA and wore at a reasonably acceptable rate.

The next area of elemental contamination observed during this research was electrical ablation or erosion from the rails of the railgun. (31, 43) One would expect this phenomenon as these rails (electrodes) see similar high currents or high energy pulses of short duration. The railgun pulse width for our experiments was normally less than 50 micro-seconds. As such, the current skin effect again plays a role and causes deterioration of the rail surface structure and subsequent ablation of material. This process was however much slower. The total surface area for current flow was much greater for the rails than the EFD. As reported, projectile railguns also suffer the same effect only to a much greater degree. (6, 37)

In addition to the current skin effect, the rails are also subjected to the detrimental effects of a very energetic arc running along their length. Although the dwell time of this plasma arc at any particular point is minute, its energy is great enough to cause near immediate material vaporization. In fact, studies (6) have deduced in the event the moving plasma arc becomes ion deficient it merely pulls rail material to sustain itself. Therefore, the total erosion effect is a combination of the

two adverse mechanisms, current skin effect and arc vaporization.

Another peculiarity of this type of system is that the plasma arc plates the rails as it moves along their length. In a sense a give and take process. Thereby, the rail surface becomes a mixture of all the previously discharged fuse materials. Figure 18 is an EDS plot obtained while examining a pure Al and Mo shot within the SEM. The impurity elements of W, Fe, Co, and Cu were found. Although the tungsten and copper could be attributed to inner EFD electrode wear the other elements iron and cobalt must have come from the rails surface. In fact, the series of shots preceding this particular discharge used an iron-cobalt based metglas as a deposition species. Using semi-quantitative (ZAF corrected) computer routines the atomic impurity percentages for this particular Al - Mo shot were found to be: Cu - 2.5%, W - 1.2%, Fe - .4%, and Co -.4%.

Without dwelling on these contamination problems, it needs to be mentioned that any system design must also contend with the atmospheric environment during the deposition. As seen throughout this thesis, many of the results involve oxygen and carbon, modifying the desired coating microstructure.

Before leaving this section, one should also realize that although the particular erosion and contamination mechanisms can not be eliminated entirely, they can be controlled. Such was the case for the inner EFD electrode. Thereby, development of a high purity system would merely involve a lower pressure vacuum chamber, some current carrying element geometrical changes, and dedication to a specific material system. That is all current carrying components could be manufactured from the same material as that being deposited, and other materials would not be introduced into the system.

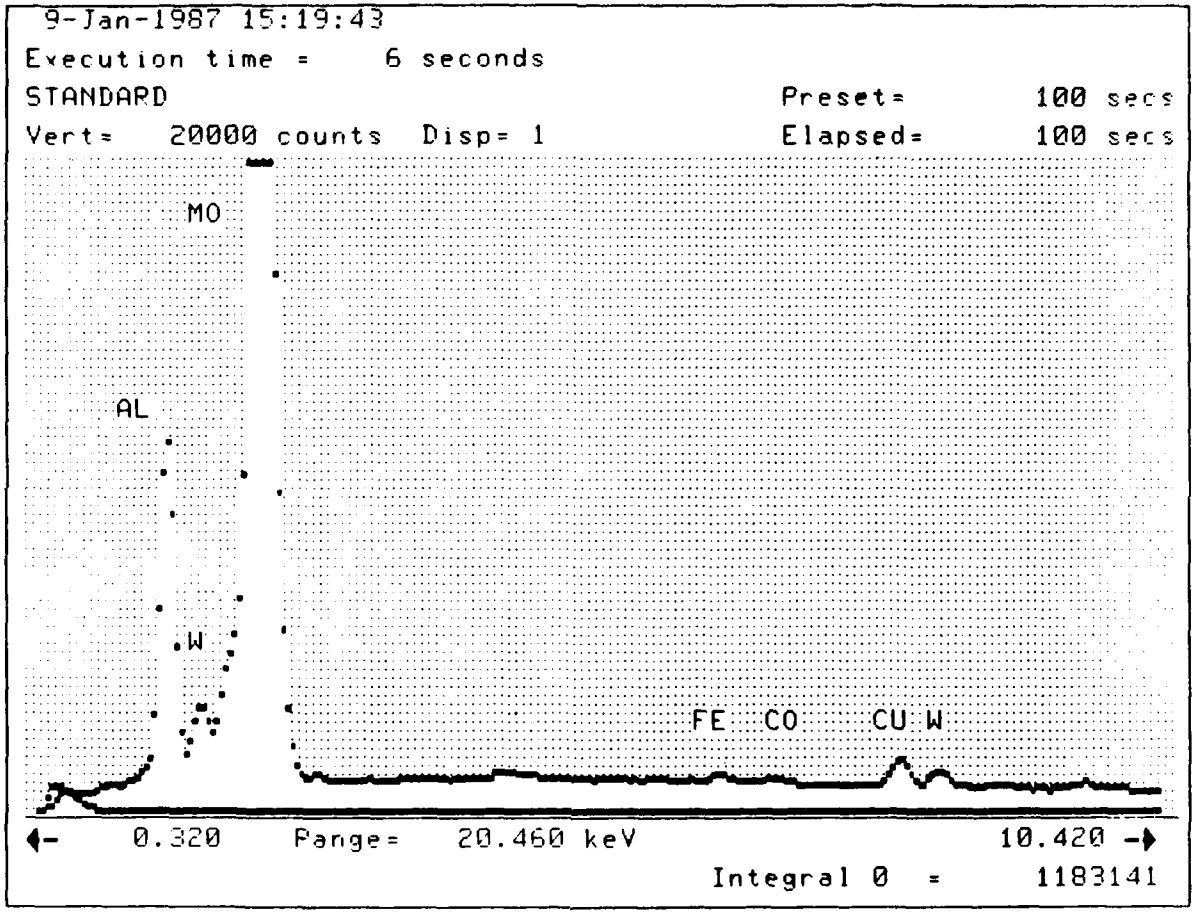

Figure 18: EDS Spectra of a Pure Al and Mo Shot,
Impurity elements identified.

EXPERIMENTAL SYSTEM EVOLUTION

The presence of liquid droplets or inhomogeneities on the surface of deposits produced by pulsed joule heating is well documented. (17, 21, 29, 31, 43, 44) In fact, Asinovskii (29) indicates that by conventional methods even in the best case the vapor phase yield hardly reaches 50%. As was seen previously, our initial experimental results only further justified their claims. Although a graded deposit may not be undesirable in all cases, a controlled homogeneous coating or film is most likely preferred. It then became the goal of the second half of this research project to produce homogeneous metallic thin films.

But before presenting my results, it should be noted that out of the group listed above, only Asinovskii (29) was successful at modifying his experiments to create a pure vapor phase deposition. His group was working with a pulsed power supply coupled to an exploding wire device. Their initial experiments involved the rapid pulsing of pure elemental wires. These deposits contained the liquid droplet phase. His idea and solution to the problem was to use composite wires. That is a refractory metal wire, Mo or W, chemically coated with a working metal such as Al or Cu. His applied energy input was then selected such that the outer coating vaporized but the base refractory metal maintained the solid state. Thereby, the current skin effect was used to his advantage.

Although his method was successful, it was not employed within this research as the quantity of material deposited was very very small, and previous attempts at combining exploding wire devices with railgun configurations were largely unsuccessful. Also, our apparatus was not set up where coated foils or the like could be used. Instead, based upon findings during the coating experiments,

modification of hardware became our antidote. Remember, the series of experiments with screening and deflector targets seemingly indicated that the lighter portions of the plasma arc could be moved about.

With this notion in mind, the first major modification entailed mounting the rails such that their long axis was orthogonal to the main stream emerging from the exploding foil device. This set up was termed the 90 degree rail configuration. (See Appendix 1, Figure A1 - 2) The presumed concept here was that the Lorentz force exerted by the rails would only be strong enough to change the momentum of the lightest portions of the arc. That is, the liquid droplet phase would go straight ahead into the vacuum chamber, while the vapor phase would turn by 90° and deposit on the target.

The first series of experiments with the new configuration involved vaporization of .025 mm Al foil at .2 mm Cu, single crystal NaCl, and Kapton tape substrates. These targets were mounted in the normal position 2.5 cm off the end of the rails, and aluminum was chosen as the deposition species because of its light weight. The capacitance discharge banks were also switched such that the stronger bank was powering the rails. The stored energy level was 6.1 kJ for the EFD, and 14.3 kJ for the rails. These first few experiments met with limited success. Although the oscilloscope traces indicated an arc between the rails, the deposits were virtually non-existent. There was some evidence of blueing at the outer edge of the targets. This indicates that possibly an 80° momentum change had taken place versus a 90° change.

Assuming that the overall concept was still good, the next set of discharges employed the use of a deflector. This non-conductive plastic deflector was mounted between the rails at a 45° angle. It was hoped the deflector would help

turn the plasma arc, and that the liquid phase would deposit upon it. The experimental set up remained the same. I would characterize the results as mixed. All 90° targets did have a deposited film on them; however a small portion of the liquid droplet phase could still be seen visually. The deflector target on the other hand was coated primarily as before with a thick rough appearing deposit. So, this method had partially worked.

The next series of experiments was designed to determine what might actually be going on during the deposition process. Several parameters were varied. The deflector was in on some shots and out on others. The stored energy level was changed consecutively from 6.1 and 14.3 kJ to 8.6 and 25.5 kJ. The banks were switched back and forth, and the rails were powered for some shots and turned off for others. It was concluded at the end of this series that although the initial idea had been good, the deflector and not the rails was playing the major role during the deposition. No shot in this series was completely free of the liquid phase.

The next idea which came to mind was that we were trying to do to much over to short a time span. The 90° momentum change was expected within the first 5 cm of plasma travel. As this plasma was traveling in excess of 10 km / sec (inferred from B-dot oscilloscope traces) the set up was considered unrealistic. This idea proved to be the key. The rails were subsequently modified to the tapered type. Appendix 2 shows the actual engineering schematic. The tapered rails were expanded to 15 cm high in front of the EFD. This would hopefully allow more time or distance for the momentum change to take place. The rails then reduced to 5 cm in height over their length to refocus the plasma.

THIN FILMS

With the tapered rails installed in the 90° configuration (See Appendix 1, Figure A1- 3), the final series of experiments began. Again, the first shot involved vaporization of .025 mm Al foil at .2 mm Cu, single crystal NaCl, and Kapton tape. This experiment was a success. All 90° targets had a thin metallic film covering them. Liquid droplets could not been seen visually or microscopically. The film actually looked like a mirror, generally indicating very fine structure. The second shot was .013 mm Ti foil and the third .025 mm Cobalt-Iron based metglas. Each of these discharges yielded an excellent result.

Figures 19, 20, and 21 are TEM micrographs and corresponding selected area diffraction patterns (SAD) of these three shots. The micrographs were obtained from the portion of the film which had been deposited on the single crystal NaCl. The films were floated off with H_2O and mounted on copper mesh grids. As one can see, the Al and Ti films were homogeneous polycrystalline vapor phase depositions. Their associated SAD patterns index as elemental Al and elemental Ti. Additionally, the SAD's and dark field micrograph of Ti also indicate random orientation. The displayed microstructure is similar to those obtained by RF sputtering, Electron beam deposition, or other commercial thin film tools. The only difference being a lack of preferred orientation, as often found with these slower processes. As these films were readily transparent to the microscope electron beam, they were initially characterized as being < 200 nm thick. The apparent difference in grain size (approximately 50 nm down for the Al and < 25 nm for the Ti), could possibly be attributed to the increase in energy level used during the Ti deposition. However, the relative quench rates and individual material kinetics sport a role.

a)

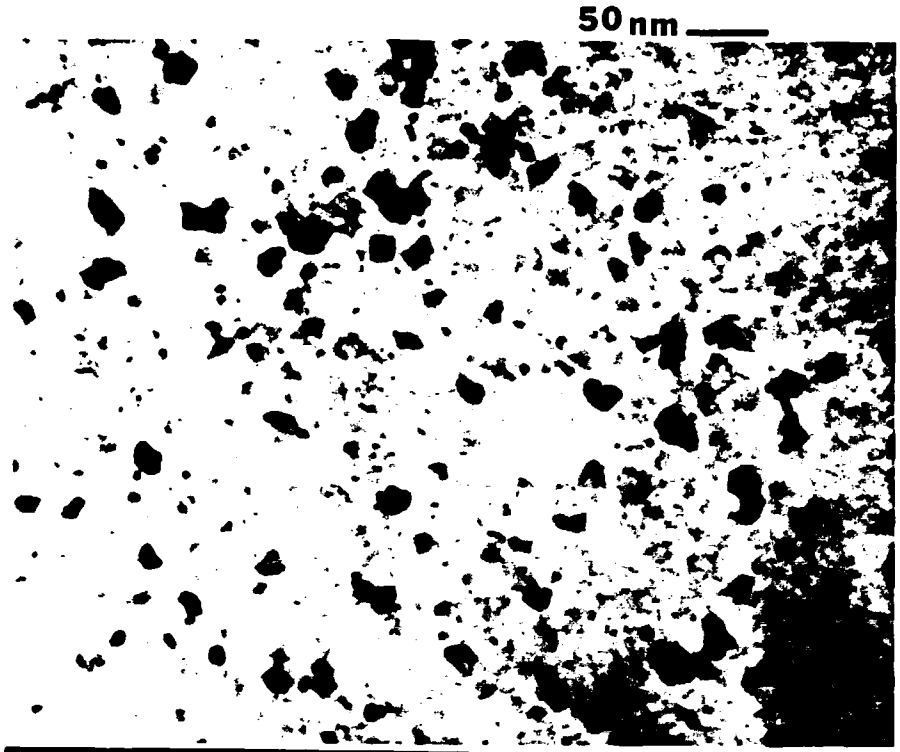

b)

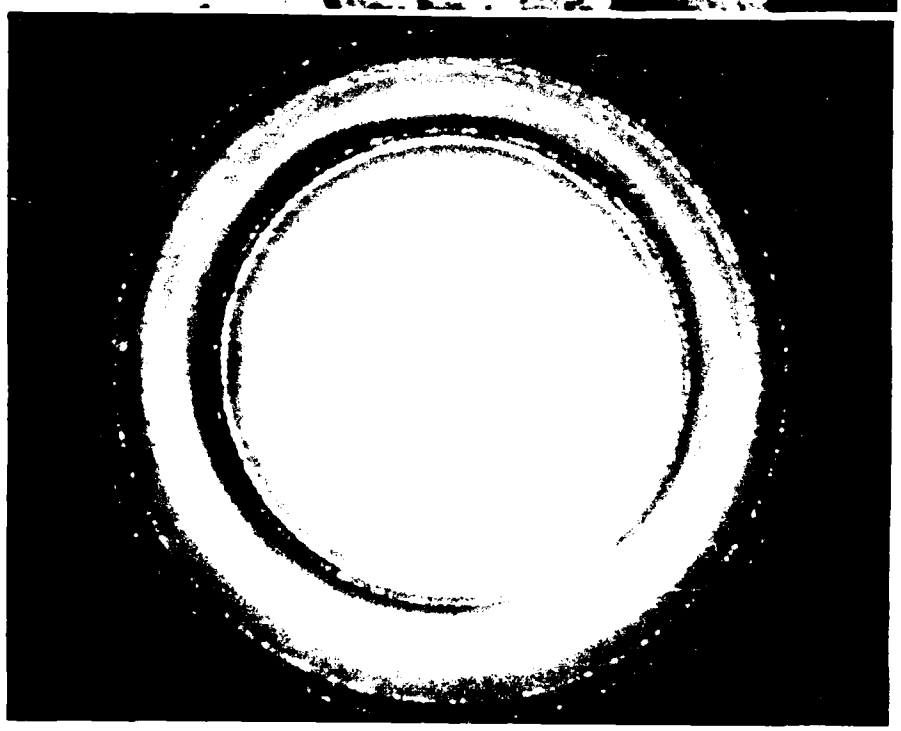

Figure 19: a) TEM Micrgraph and b) Selected Area Diffraction Pattern of Shot # 157 (pure Al discharge), Tapered Rails at 90°.

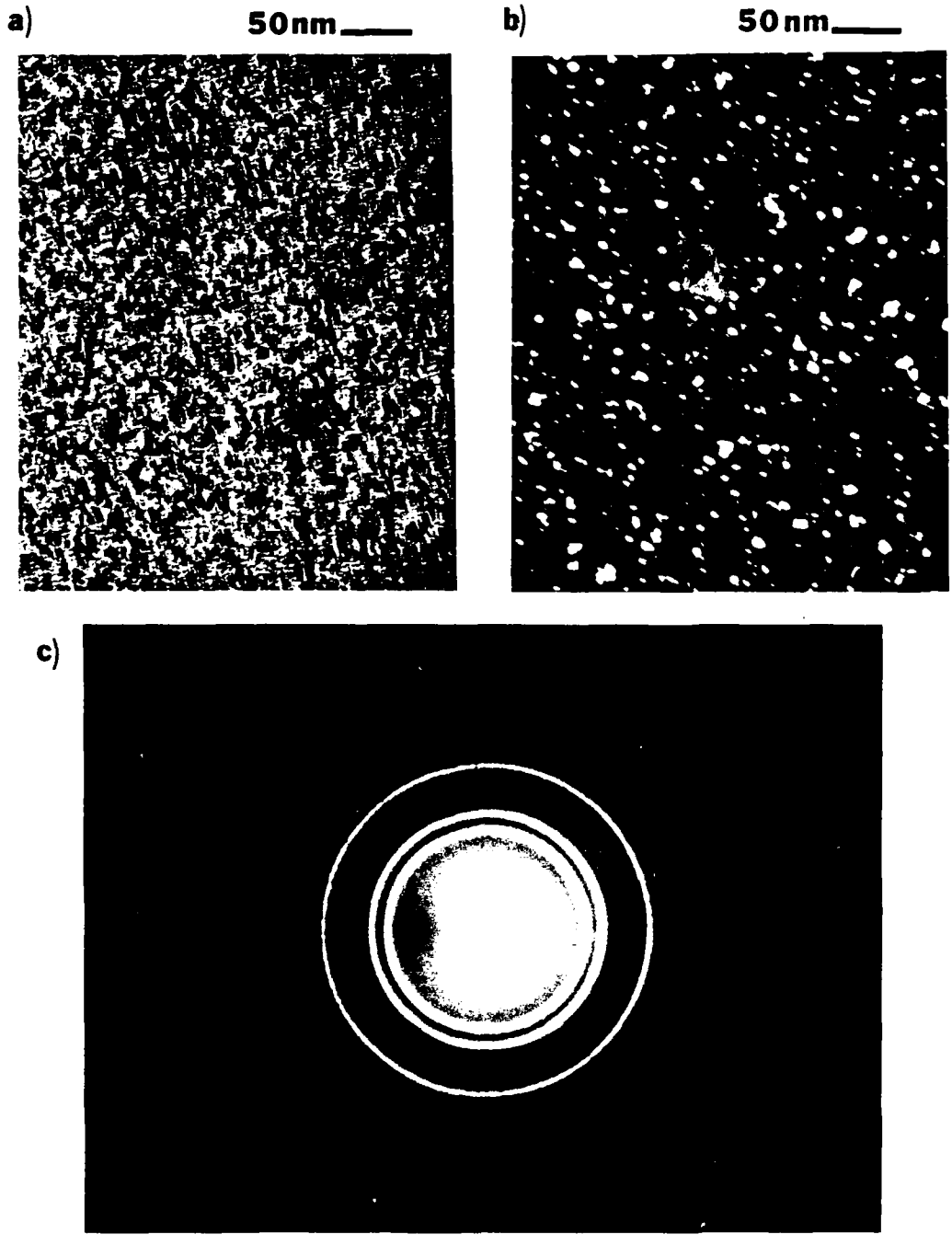

Figure 20: TEM Micrographs of Shot # 158 (Pure Ti Discharge)
a) bright field b) dark field c) Selected Area Diffraction Pattern.

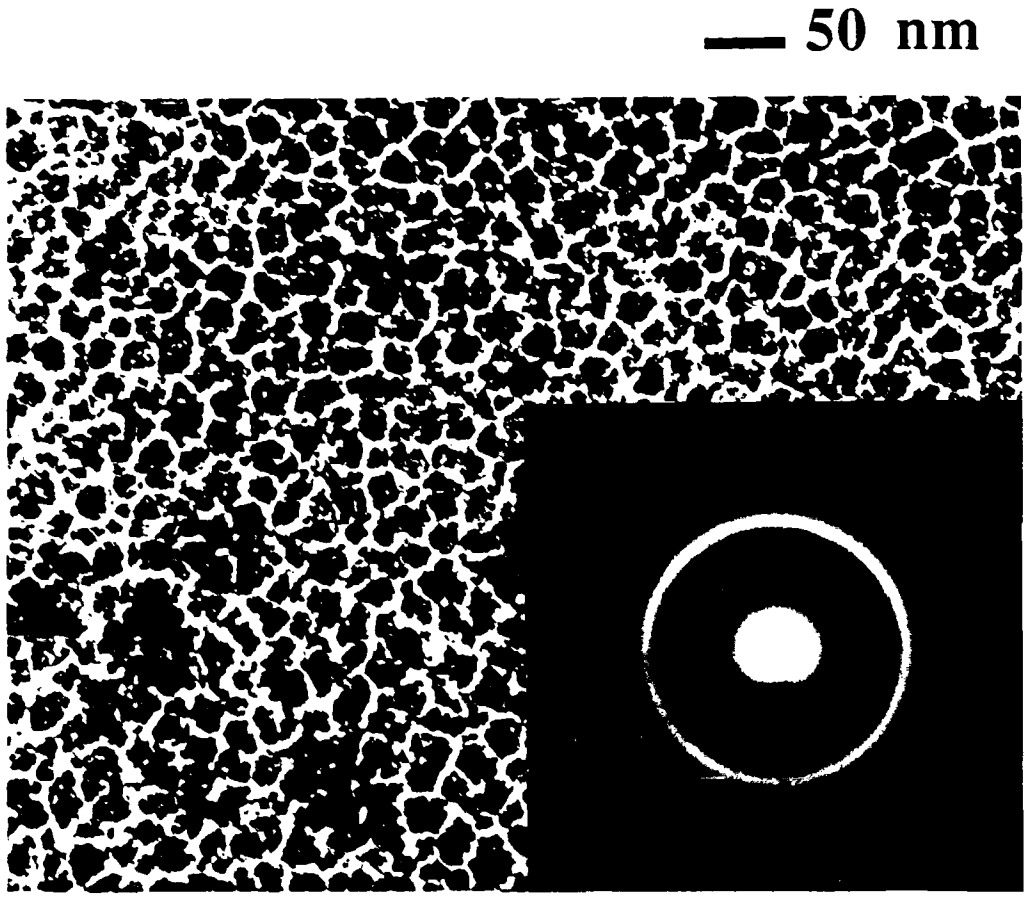

Figure 21: TEM Bright Field Micrograph and Corresponding SAD Shot # 156 (Cobalt Based Metglass) Deposition maintained the non - crystalline state. Film also shows a modulated or phase separated structure.

The third metglas sample also provided an interesting result. Though the material had transformed from the solid to vapor state during the deposition process, the end result was again a glass structure. This points to a quench rate on the order of 10^6 K / sec. (45, 46, 47) Its cellular appearance results from short range phase separation. Typically the lighter regions indicate areas where the low atomic number elements are most concentrated and vice verse for the dark regions. Phase separation, cellular structure, and short range ordering are well documented across the metallic glass literature. (47)

Now, not only does the system have the capability of vapor phase deposition, but from the micro-crystalline grain structures obtained and subsequent glass production, it also shows promise as a rapid solidification tool for materials not easily liquefied.

Given the success with the Al and Ti discharges, the next deposition set, 5 total, was aimed at plasma mixing the two elements. The aluminum content was varied from approximately 50 -75 atomic percent over the series. The energy level remained constant at 23.0 kJ for the EFD and 7.8 kJ for the railgun. The targets were Kapton tape, NaCl, and .2 mm Al.

All five discharges produced excellent films with mirror like finishes. The film containing 75 at % aluminum was a homogeneous polycrystalline mixture of elemental Al and Ti. Again, no preferred orientation was seen and grain size was < 30 nm. On the other hand, the four discharges with 50-66 at % aluminum were found to be mostly non- crystalline. Figure 22 a,b,c, are the electron micrographs of one of these discharges. As seen, the SAD shows diffuse scatter and the dark field image virtually an absence. This is an indication of possibly non-crystalline, short range ordering. Due to the unlikeliness of this result for pure metals, these four

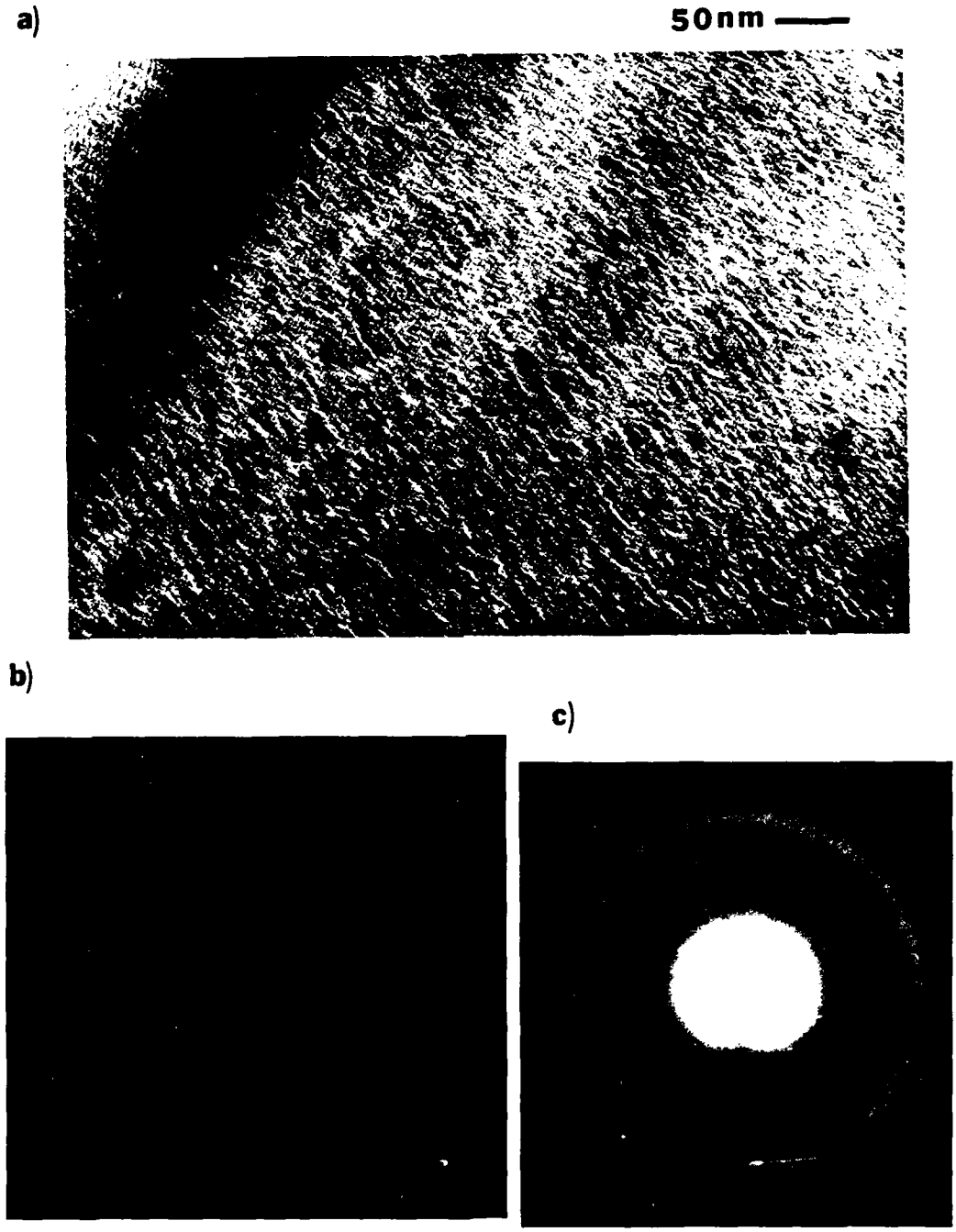

Figure 22 : TEM Micrographs of Ti - Al Shot # 160. Film = 95 % non - crystalline. a) Bright field image - darkened region is a bend contour b) Dark field image - lack of crystallite reflections c) Selected area diffraction pattern - only diffuse scatter.

specimens were further examined with EELS in the STEM. The obtained EELS spectra, one example Figure 23, indicated the presence of oxygen and carbon within these films. Also, as we were able to get a good EELS signal, the samples must have been between 50-100nm thick, 1 to 2 mean free path lengths for plasmon losses (48).

To further characterize the result, the samples were depth profiled using Auger spectroscopy. The profiles were consistent and as seen in Figure 24 , the Ti seemingly pulled carbon from within the vacuum system and Al pulled oxygen. The individual spectra, Figure 25, also showed that the Al peak (1386 ev) had shifted about 7 eV to the lower energy side. This may additionally be an indication of Al and O short range order. The crystalline Al_2O_3 peak (1380 ev) is 12 eV lower than elemental Al (1392 ev). The carbon peak also changed its feature as one sputtered away from the surface. The surface carbon peak had the characteristic elemental shape, whereas the depth peak showed fine structure plasmon losses. The presence of plasmon losses off the carbon peak generally indicates carbidic nature; however at times, this change is a result of the ion sputtering process itself. In any case, as these lighter elements can reduce the surface mobility of the heavier metals, the non-crystalline result is now somewhat understandable. In fact the role of carbon in stabilizing amorphous Ti films was presented by Potter. (49) Likewise, for our experiments the Ti - C couple must have been important. As previously noted, the lowest concentration Ti discharge (beginning at % 25) reverted to polycrystalline material. Lastly, the films were well bonded to the Al substrates.

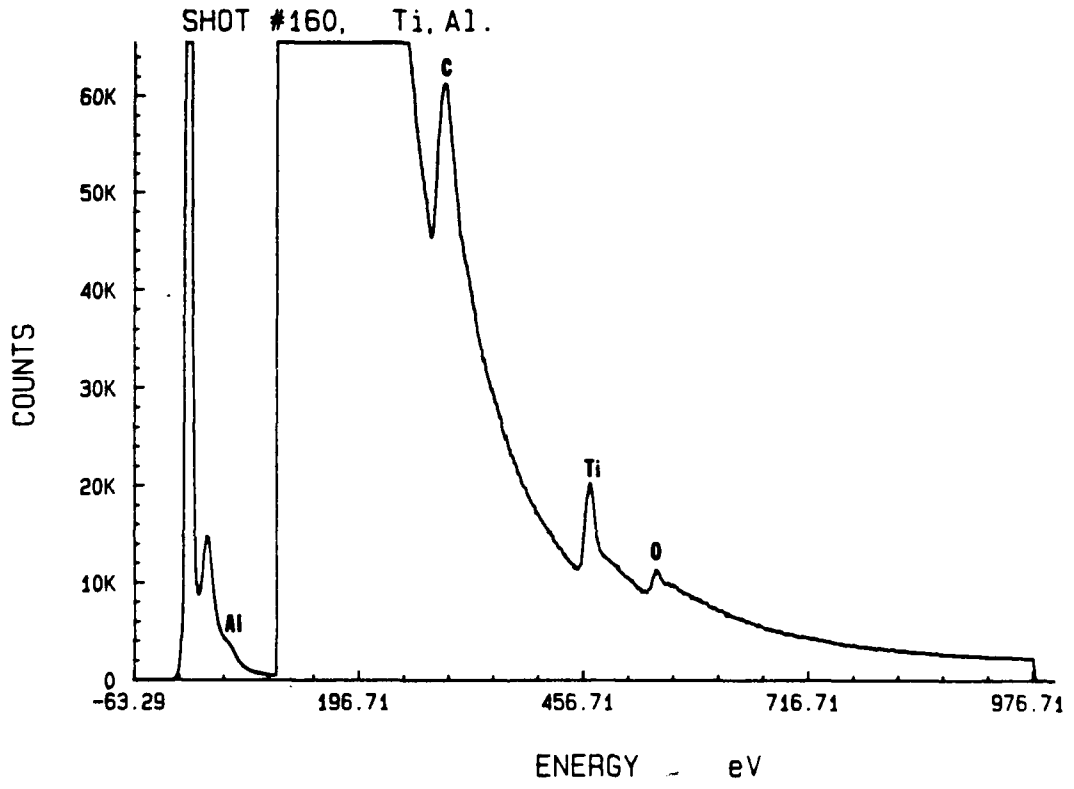

Figure 23 : EELS Spectrum of Shot # 160 , Spectrum shows presence of elemental oxygen and carbon within the film structure.

a)

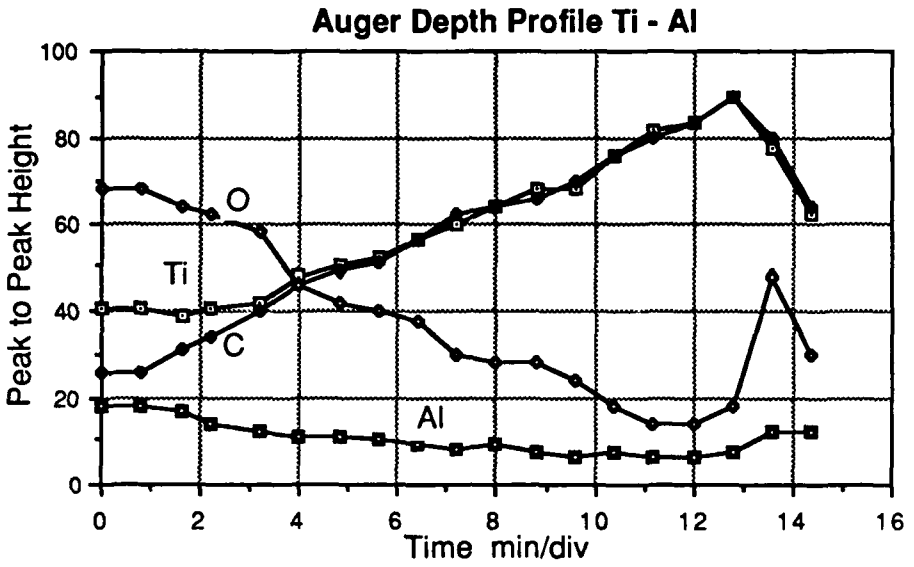

Ep 3.0 kV, Ip 375 nA, Vmod 3, Vmult 1050, RC .3/5, SENS 20X, 5 Feb 87;
Etching: Ep 2.0 kV, Ie 25 mA, rate ≈ 10 nm/min, raster 2 x 2 mm

b)

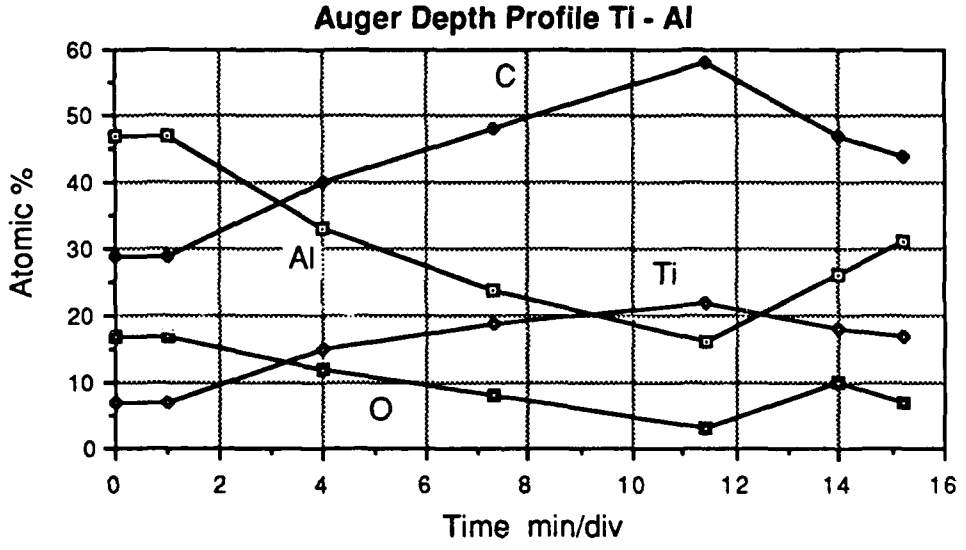

Figure 24: Auger Depth Profiles For Shot# 160-7C a) Peak to Peak heights b) Peak to Peak heights converted to Atomic percent.

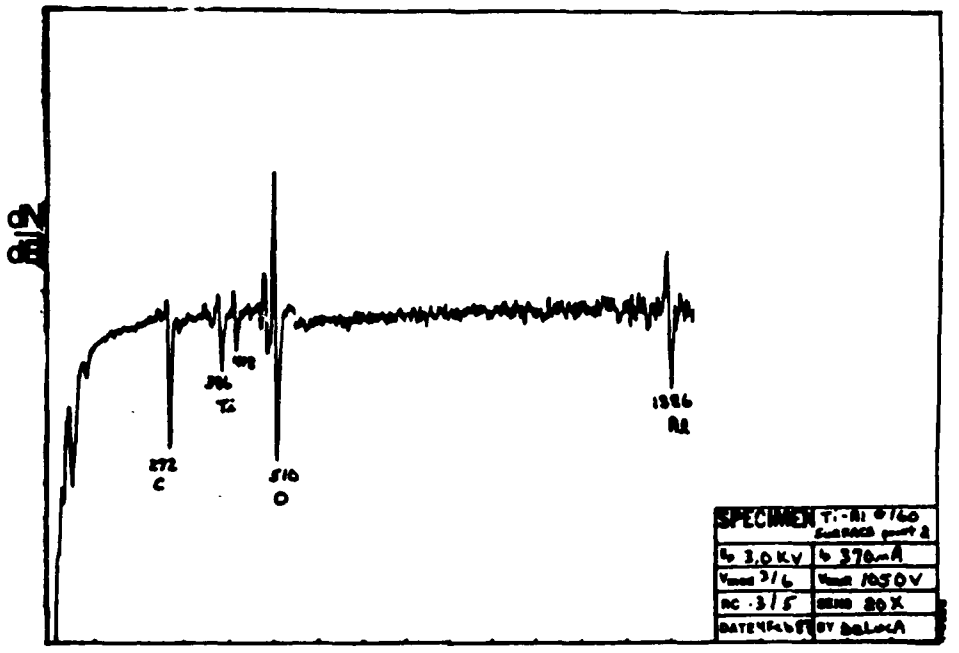

Electron Energy eV

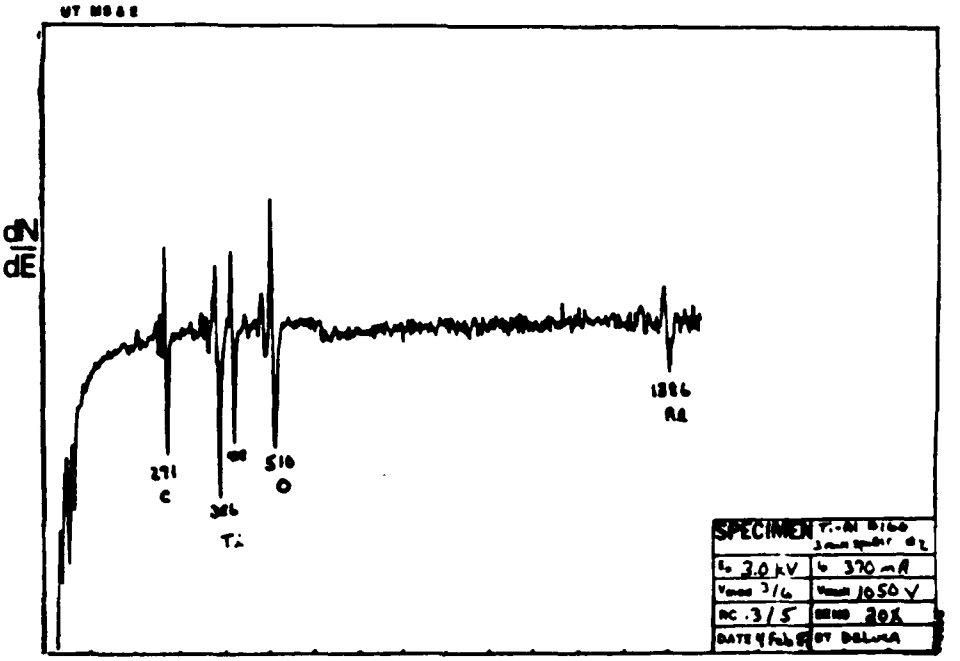

Electron Energy eV

Figure 25: Auger Spectra of Shot # 160, top - surface spectrum, bottom - spectrum after 3 minute sputter.

The final series of thin film depositions, entailed the plasma mixing of Al with Mo or W. The energy level and targets remained the same. The aluminum content did change and varied between 33 and 66 at %. The overall results were mixed yet most informative. The initial shots with 33 at % Al and either 67 at % Mo or W, lead to the unwanted reappearance of the liquid droplet phase. From EDS analysis, these droplets were found to be either Mo or W. However, as seen in Figure 26 a distinct droplet size difference is noted between the Mo and W shots. On close examination, the size difference is roughly a factor of two, as is their density. Thereby, it was hypothesized, in the event the plasma arc was deficient of vapor phase ions, a drag type process occurred to sustain current flow. This deficiency resulted from inadequate energy input. Also as the Lorentz acceleration is finite, the drag process was mass selective.

Another interesting result came out of one of these shots. Figure 27 shows a portion of a 33 at % Al 67 at % Mo film which tore like paper. Examination indicated a one to one correspondence across the tear and also that the light portion was the underside. High magnification of the light region showed phase separation and diffuse scattering for diffraction, Figure 28. Again an indication of a glassy structure. Also as one can see, towards the right of the bright field image and in one preferred direction on the SAD, microcrystals and diffraction spots are present. The film is actually graded from non-crystalline to polycrystalline as one moves up to its surface. Thermodynamically, the quench rate slowed as the material deposited. EELS analysis was performed on the light glassy region, seen in Figure 28. The stripped EELS signal (Mo energy range) , Figure 29, showed the presence of oxygen, in fact the waveform shape was very similar to that obtained from crystalline Mo oxide. Again, presumably the oxygen and probably carbon restricted the surface

a)

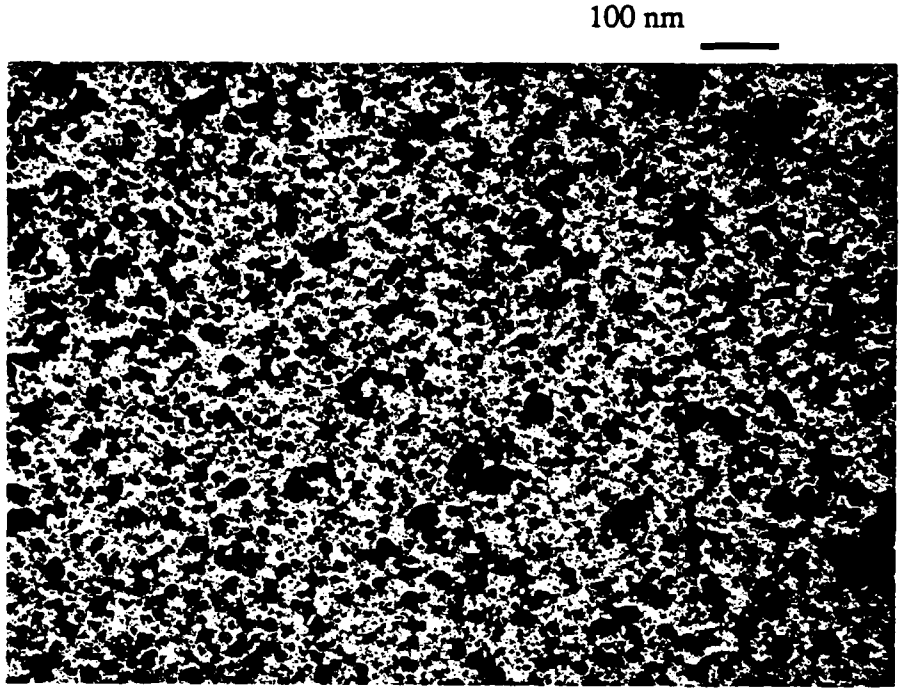

b)

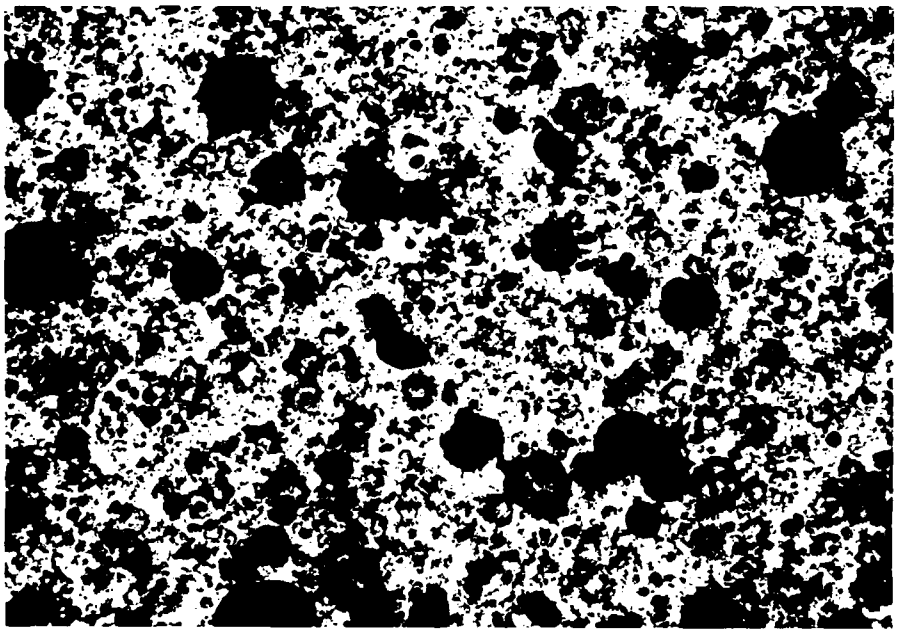

Figure 26: TEM Micrographs of a) Shot # 185 (Al and W) , b) and Shot # 189 (Al and Mo). Notice the difference in liquid droplet size.

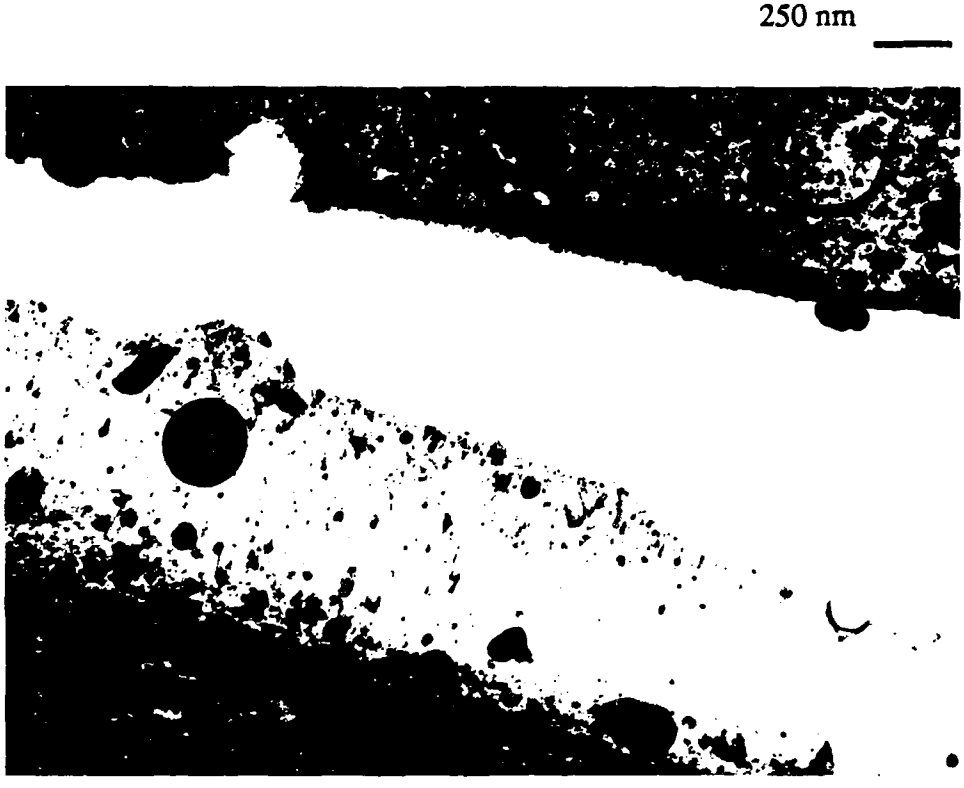

Figure 27: TEM Micrograph of a Fractured Portion of Film. Shot # 189
(Al and Mo)

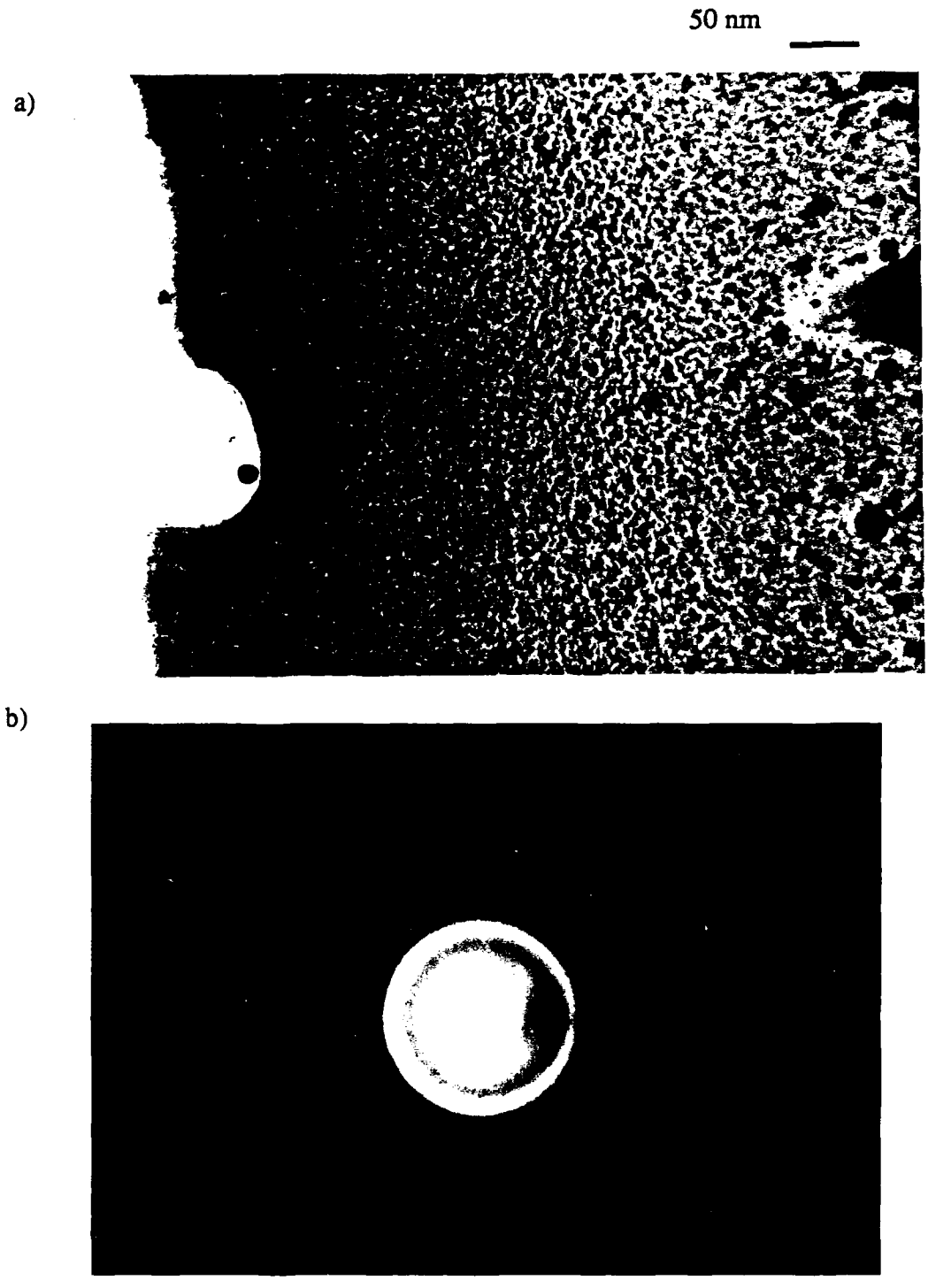

Figure 28 High Magnification TEM Micrograph a) Light underside region of Figure 27. Phase separated, modulated structure. b) Corresponding SAD

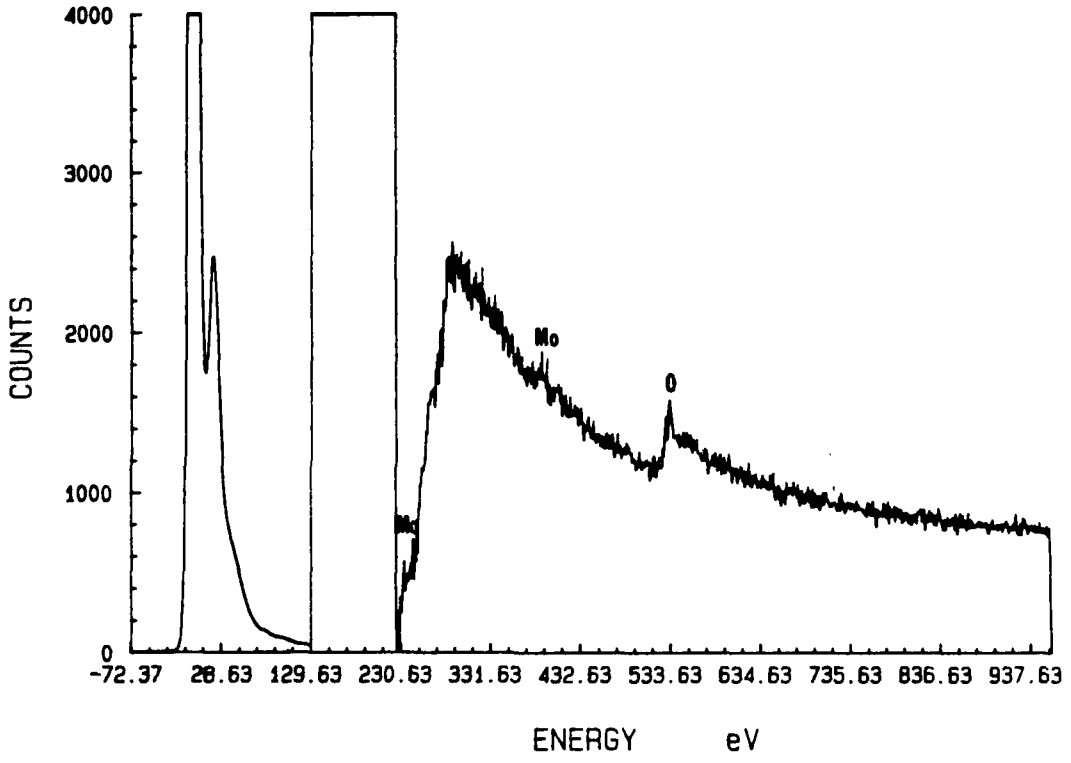

Figure 29: EELS Spectrum From Glassy Region of Figure 28.
Spectrum indicates presence of elemental oxygen.
Overall waveform shape similar to crystalline Mo oxide.

mobility of the heavier Al and Mo ions. Semi-quantitative depth profile Auger analysis indicated between 10 and 18 at % oxygen. After some comparative calculations, the environmental oxygen present between the rails (approximately 2.0 x 10^{-9} gm moles) , just prior to the discharge, does not account for all that found within the samples. Thereby, oxygen is being gathered from the surrounding vacuum area, and in all likelihood from the native rail and foil surface oxides, as well as their surface adsorbed H_2O.

Next, examination of the 50 - 50 at % couples lent more justification to the above mentioned hypothesis concerning the resolidified liquid phase. The liquid droplet phase was much reduced in these samples, as seen in Figure 30. This stems from the fact that more vapor phase aluminum was present. Also, as the dragging mechanism component was less, so to was the liquid droplet size.

Finally, as one might expect, when the Al content was raised to 66 at % homogeneous polycrystalline metallic thin films were obtained. No liquid droplets were present. Figure 31 is an example micrograph of an Al - W shot. The ring diffraction pattern from this particular shot was also noteworthy. No tungsten rings were indexed. The pattern shows a pure elemental Al matrix. Semi-quantitative EELS across all portions of the film indicated between 8 and 12 at % tungsten. The equilibrium solubility of W in Al is .1 %. This leads to three possible conclusions: the tungsten grains are so small that significant diffraction is not occurring, or the tungsten atoms are along the Al grain boundaries, or the structure is very non-equilibrium. To reduce these possibilities, convergent beam micro-diffraction and EDS across the Al grain boundaries was attempted . Due to the tiny grain size < 25 nm , this task proved to be beyond the capability of our STEM. A null result was obtained.

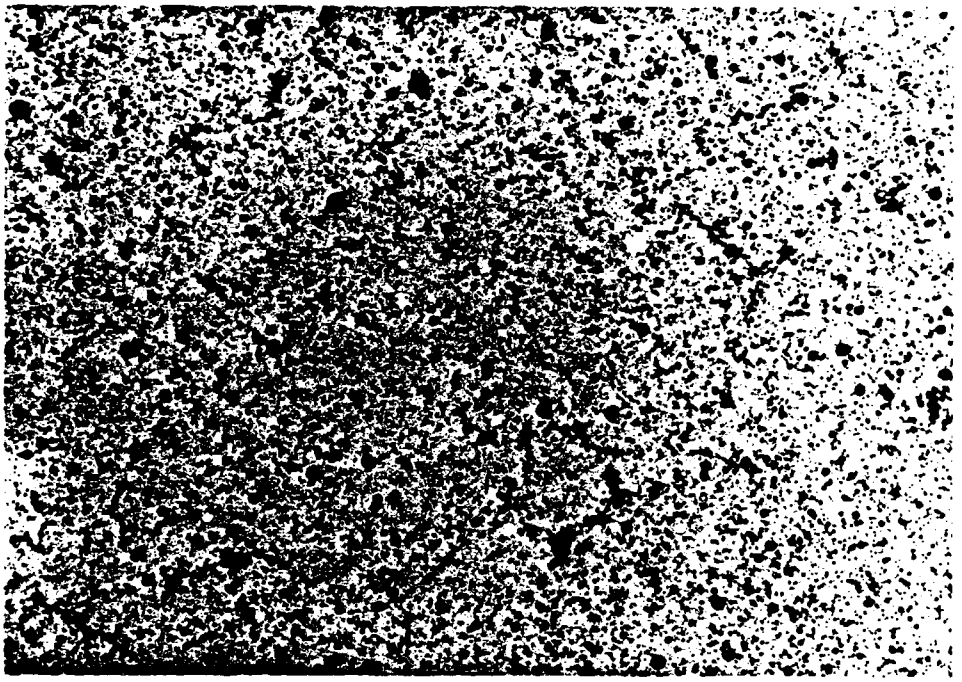

Figure 30: TEM Micrograph of 50 - 50 at % Al - W Couple.
Liquid droplet phase smaller and much reduced.

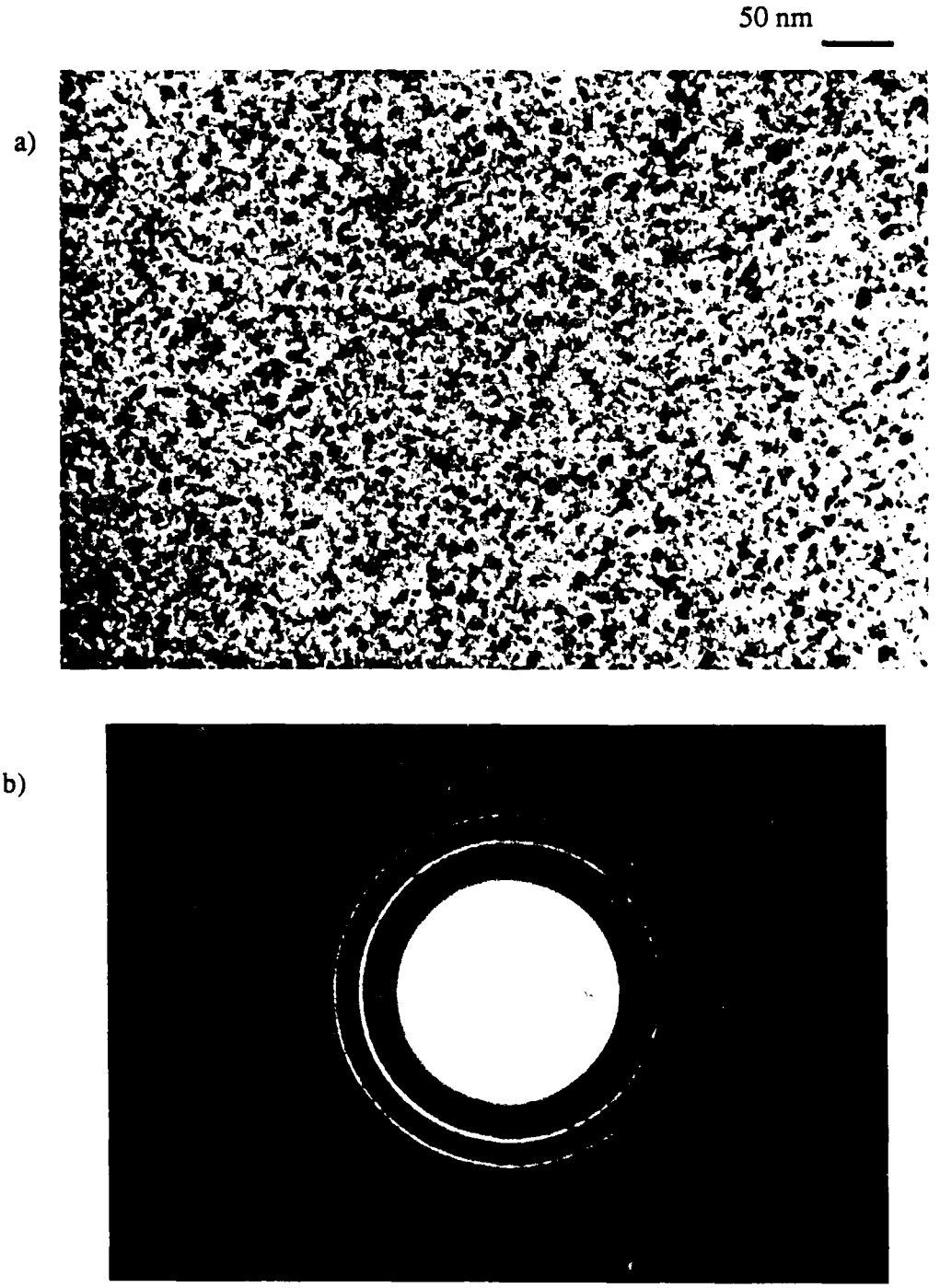

Figure 31: TEM Micrographs of a Produced Homogeneous Thin Film
66 at % Al, 33 at % W (Starting percentages). a) bright field image
b) SAD - indicates Al matrix only.

Now, although this series of experiments, as in the coating section, led to no intermetallic 2nd phases as initially hoped, it taught us a great deal about our new deposition process. First, the process requires a minimum amount of conductive material. Second, if the vapor or plasma phase is insufficient to fulfill this initial requirement, a dragging mechanism begins to pull tiny liquid droplets. And third, this mechanism was found to be mass selective. These observations lead to the deduction that the whole process is somewhat controllable.

Upon completion of this final series of thin film experiments, the railgun apparatus was dismantled for examination. Like the previous coaxial rails, the tapered rails had been plated by the deposition process. In fact, as seen in Figure 32, this plating allowed for near direct observation of the plasma's behavior. Apparently the rails had been just high enough. The plasma stream progressed across most of their height before undergoing its directional change. One can also see the plasma seemingly expanded as it traversed the rails length. This accounts for the final uniform surface coverage. Its ironic that the undesirable aspect of surface rail coating, led to a good result. That is, it gave us a better overall understanding of the system in near pictorial form.

This concludes the experimental deposition results. The final section of this chapter deals briefly with the diagnostic instrumentation findings.

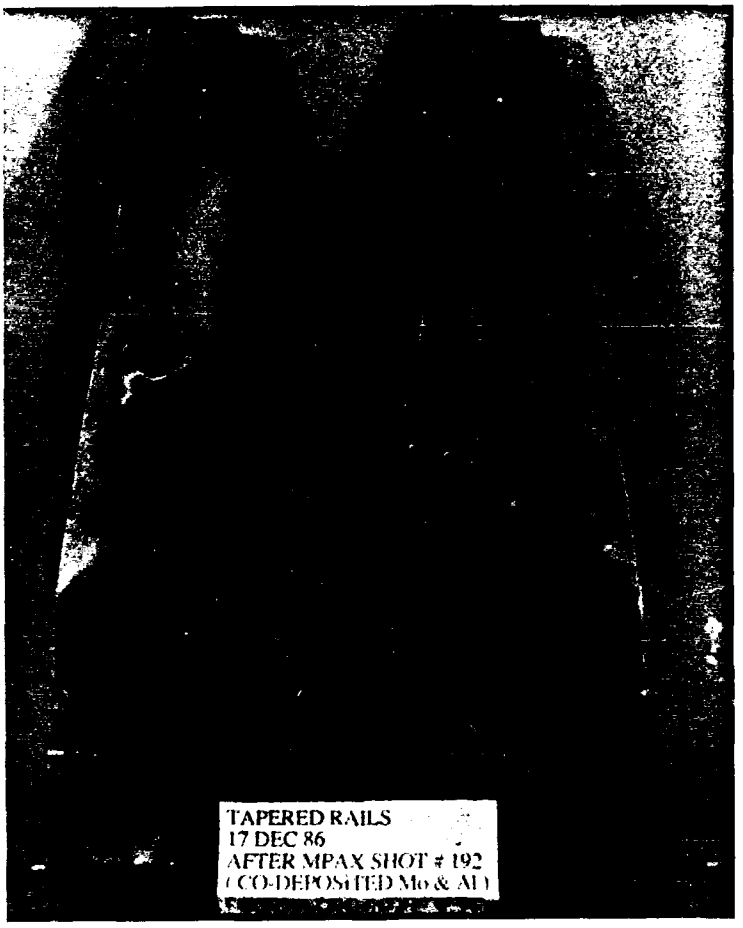

Figure 32: Photograph of Tapered Rails After Completion of the Thin Film Deposition Series.

INSTRUMENTATION

Though not a major impetus of this research, a concerted effort was made to obtain diagnostic information about the deposition process. As such, a deposition experiment was not conducted if the basic current and voltage levels could not be obtained. However, several experiments were accomplished without any plasma velocity information.

As described in the experimental set up, current and voltage levels for both the EFD and railgun were acquired using Rogowski coils and resistive voltage dividers linked to Nicolet oscilloscopes. For these measurements, a scope resolution of 500 nsec / point was found to be satisfactory. An oscilloscope trace of these levels is seen in Figure 33.

This trace is from coating experiment # 71. As one can see the peak exploding amperage was roughly 220 kA, and the peak gun amperage was about 90 kA. The peak voltages were 1400 and 900 V respectively. These voltage and current traces were consistent from shot to shot, and this figure portrays a good representative. The only difference would be scaling. That is, peak exploding amperage ranged from approximately 150 - 350 kA, and gun amperage from 75 - 150 kA, across the entire research project. On the other hand voltage varied from about 750 - 1500 volts for the EFD and 500 - 1000 volts for the railgun. Time to peak height varied little and was typically 20 microseconds at the beginning of the project, and then 18 microseconds after the system inductance improvement. With regards to this particular discharge, the starting stored energy level was 12.5 kJ for the EFD and 4.7 kJ for the railgun. The other traces of this project naturally changed relative to the starting input.

Now, on initial observation, one should also note that by approximately 80 microseconds the gun voltage is near zero. This indicates that the deposition is basically complete. No arc remains between the rails. As you will see later, the B dot signals have also died by this point. Thereby, the whole process is exceeding fast by any existing deposition scale. With regards to the existence of exploding voltage at this point in time, this is really an artifact. Due to the close proximity of the two EFD electrodes continual arcing occurs until energy depletion. This consequence was

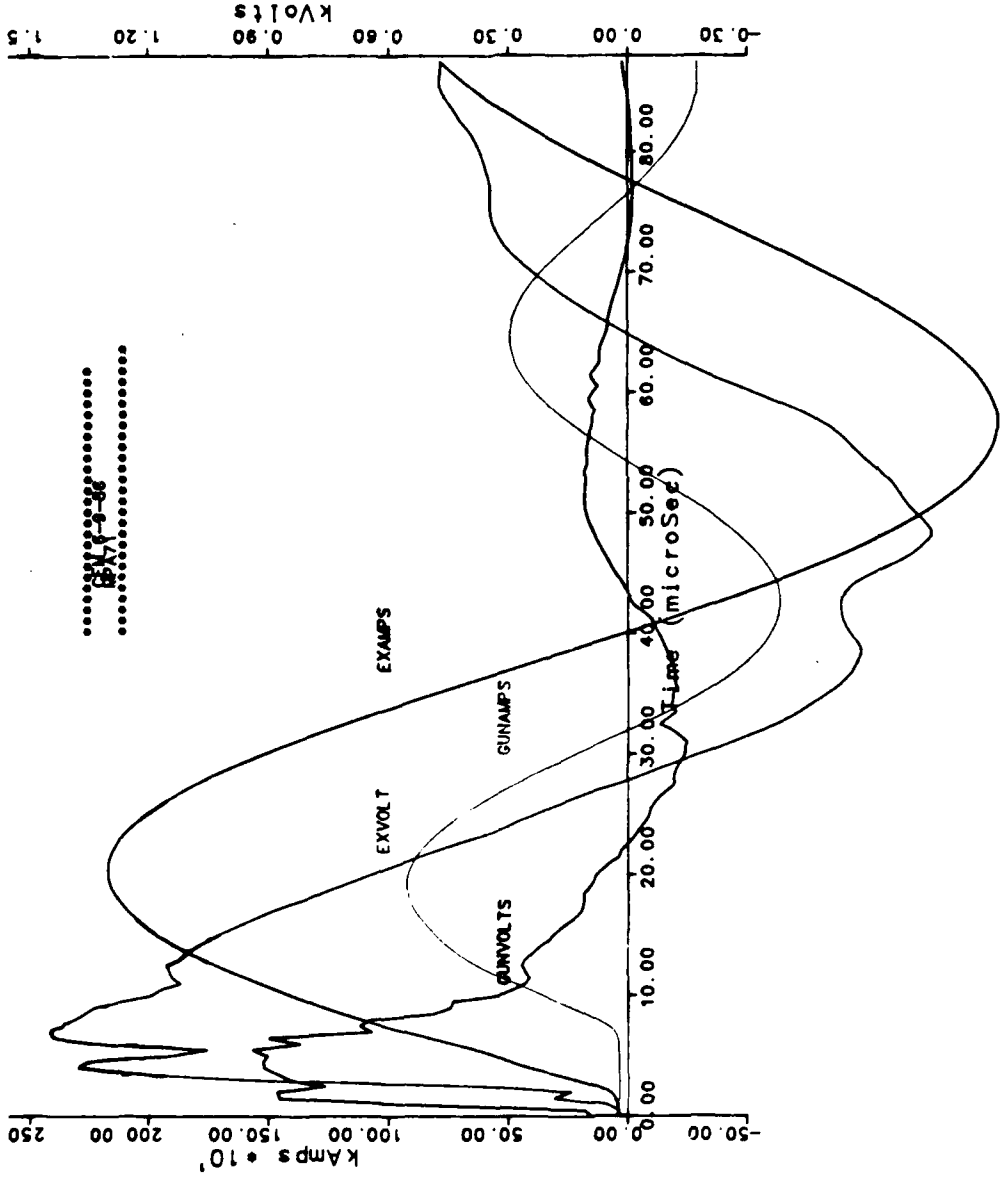

Figure 33: Oscilloscope Trace Showing Typical Amperage and Voltage Levels.

seen for over a hundred discharges and may be an additional reason for our erosion problems.

Another aspect of this trace which is noteworthy is its overall damped oscillating nature. Although a DC circuit, its appearance is likened to AC. This is known as capacitance ringing. It realistically occurs due to the short time scale involved. The bank is attempting to give up all its energy immediately, but due to system resistance a finite time scale is required. This back up leads to a change in polarity. What is interesting is that despite the polarity change, the Lorentz force is always down the gun. As the current changes direction, the magnetic field also changes its orientation. One detrimental result of this process is the plasma arc coasts during the transition. Uniform acceleration is not really possible with single capacitance banks. Projectile railgun circuits compensate for this effect by using multiple sequentially discharged banks and what is called a crowbar circuit. This circuit chops the release of energy at the first polarity change. By that point the second bank has reached near peak energy release. The sum total is a fairly even acceleration. This type of set up was however well beyond the practical limits for this initial exploratory research.

Perhaps the main reason for collecting this data was to determine the systems energy efficiency. That is, the ability of the system to convert stored energy into resistive heating energy within the EFD, and plasma arc energy between the rails. The efficiency was calculated manually from these traces by incrementally summing the power input (V x I) versus time across the first 80 microseconds for the railgun, and until the first polarity change for the EFD. The overall energy efficiency of the railgun was found to be between 7 and 15 %. The exploding foil device ranged higher at 15 - 25 % efficient. Although these numbers seem fairly small, they are

well within the range reported by others. (6) Remember, any system like this involves a great deal of losses due to resistive heating of all current carrying components. The gun efficiency is also lower here than the EFD as the moving plasma arc involves an associated direct power loss.

The second diagnostic area was an attempt to determine the plasma velocity during the discharge. Knowing this velocity, one could better characterize the deposition energy realm. This however proved to be a major undertaking, and although we did achieve results in this area, I would consider them ball park figures. In fact, only about one in ten shots provided a usable signal.

The initial hope was to get a substantial deflection of the B dot signal as the plasma arc passed its point along the rails. However, the B dots were just not very consistent. Several different types and configurations were used throughout the project but no specific good arrangement was found. At times even a scope resolution of 20 -50 nsec per point seemed unacceptable. This was in part due to our maximum B dot separation limit of 15 cm. In general, the signals were found to be overly complex and hard to infer velocity from. When minimum shielding was applied, the signals became to weak. Figure 34 is perhaps our best result from the coating series of experiments (coaxial rails). These particular B dot signals, shot # 46, yielded a near one to one correspondence between them. By matching point to point time differences, an average velocity of about 45 km / sec was calculated. Other signals within the group of coating experiments pointed to an overall range between approximately 30 and 50 km / sec. As projectile railguns have reported accurate velocities of gram armatures to near 10 km / sec, (7) our plasma arc range is at least realistic.

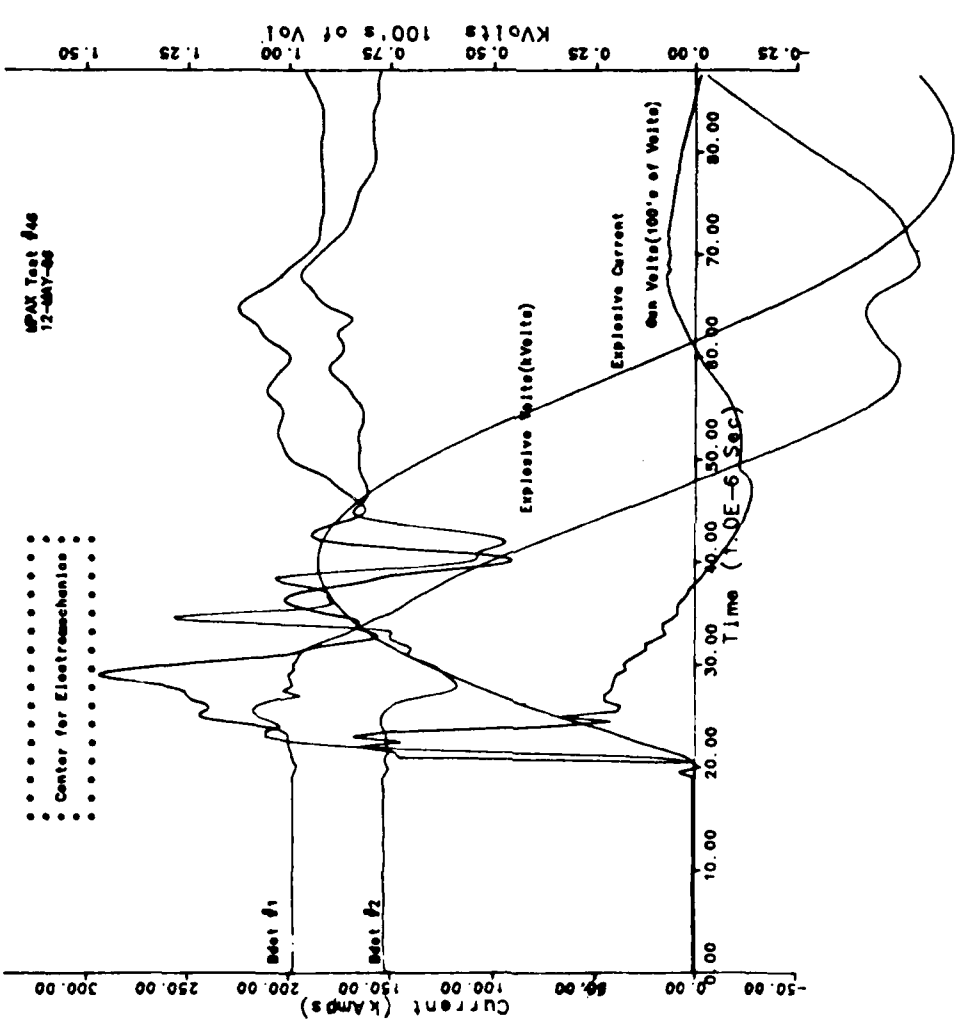

Figure 34: Oscilloscope Trace Showing the Corresponding Plasma Arc B dot Signals

During the late stages of this project, the B dot probes were replaced with photoelectric transistors. We were now attempting to accomplish the same result with optics. The photoelectric transistors were used first with the tapered rail configuration. For this railgun configuration, the signals were excellent. One distinct signal rise and fall was seen from each transistor. The signal obtained from the second transistor was much broader than the first. This indicates the plasma arc lengthens over time. This result is fully expected as the heavier portions of the arc, an example ion clusters, must fall to the rear. By measuring the time difference to peak height and given their 25 cm displacement, a velocity of 4.6 km / sec was calculated. Over a series of four similar shots, same material - same energy, the spread was only .2 km / sec. I feel confident of this result. The order of magnitude difference here is very explainable. Recall, for the thin film depositions, most of the plasma must first change direction by nearly 90 degrees. In a sense, the arc was starting from near rest versus approximately 5 - 10 km / sec coming out of the EFD. Although these discharges were actually the end of the project, three experiments were reaccomplished with the coaxial gun to test the new photo-transistors. As somewhat expected, the transistors themselves (rated as approximately 5 microsecond rise time) did not have the resolution to function in this configuration. Their signals were right on top of each other, another indication of the much greater velocity range in the straight ahead mode.

CHAPTER 5

SUMMARY

The rate at which technology has advanced over the last thirty years has been truely phenomenal. Even those of us educated during this time period often shake our heads in amazement. Yet in spite of all this advancement, the opportunity for improvement still exists. In fact without continued improvement, specifically in the materials area, much of the new technology will stagnate. The need for smaller, faster, lighter, and stronger has moved materials research into a preeminent role. Now, not only are new materials required but new means of producing them and also processing them. Therefore, the overall goal of this thesis was to improve upon a past production and material processing method.

More specifically, this study addressed the general area of material surface coatings. As indicated in the introductory section, there are several commercially available coating tools. However, each operates within a specific realm, and along with its advantages often come disadvantages. Recall, plasma spraying sometimes lacks good adhesion, thin film technologies are often time consuming, and implantation requires post annealing treatments to alleviate surface damage.

In an attempt to fill some of the voids in the present coating technology, Brown (17), NASA (31), and CEM conducted deposition studies using electromagnetic propulsion (railguns) and new pulsed power supplies. Studies of a similar nature have also emerged from Russia and Poland. Although by no means a panacea, each of these efforts showed promise for a new deposition technology based upon these electromagnetic railguns and or pulsed power application. This research

was thereby founded upon the best efforts of the above. The deposition system itself was designed by CEM and incorporated all their prior knowledge. The major beginning difference was the use of separate capacitance energy banks to first produce the plasma, and then accelerate it.

The incorporation of a new exploding foil device to generate the plasma material yielded positive results from day one. By shot number 10, the machine was found capable of producing full coverage uniform deposits of 20 μm thick. This was accomplished by merely adding a second foil within the EFD and incrementally stepping up the energy level. From this point, the project took on a broad nature to find the best suited realm of operation. All total over 15 material systems were investigated and several findings were detailed.

The first major finding was the coating process produces a graded deposition. The initial material down is primarily vapor phase. This is followed by tiny then larger liquid droplets to form a build up type coating. As such, the coatings show some porosity. The coating thicknesses ranged from 10 - 200 μm. It was also seen, by continually increasing the foil thickness at constant energy, the vapor phase portion of the deposit could be eliminated.

It was next found that distinct surface morphology changes occur with varying target placements. A sweeping or directional coating was obtained by orienting the target parallel to the plasma stream.

Surface adhesion was characterized as overall very good. Most coatings could not be scrapped off the substrates. The best results were obtained by using a high melting temperature deposition material against a low melting temperature substrate. Also, abrasively cleaning the substrate just prior to evacuation made a noteworthy difference. And finally as expected, an increase in energy level definitely

improved adhesion. In fact, in the extreme energy case substantial surface modification occurred. The typical plasma arc contained enough energy to completely vaporize .025 mm Al targets, and although the process showed little direct proof of ion implantation, the surface and deposition materials could be readily mixed by a heating, melting, and resolidification action. The end result being a completely new surface. Intermetallic second phases between Al and Cu were formed by this method.

From this result, it was concluded that mixing in the plasma, vapor, and liquid phase should be possible. Multi-foil mixed element couples were attempted. The Al - Cu system produced positive results. Three different intermetallic compounds were formed, $CuAl_2$, Al_4Cu_9, and $AlCu_3$. This effort was expanded to include Al - Mo, Al - Ti, and the Al - W systems. Despite the previous success, intermetallics were not formed for these systems. Rather due to the internal environment and presumable the free energies involved, various oxide compounds formed. However, even at reduced energy levels, good adhesion was noted. As the substrates were Al, lattice matching across the interface may account for this result.

In addition to the environmental contamination of oxygen listed above, the system hardware proved to be a contaminating source. Rail erosion resulting from the skin effect accounted for impurity levels of 1 - 2 at %. Also, at the beginning of the project, gross contamination occurred from the inner electrode of the exploding foil device. This was corrected by remanufacturing the electrode out of Elkonite 67 % W, 33 % Cu.

The final coating experiments entailed the use of foil packets filled with powders. The plasma arc successfully pulled and codeposited the metal and

powders. The deposited powder size was found to be smaller than the original starting size.

At this point in the research, approximately shot # 80, the system and its initial capabilities were well understood. The deposits within each material group became very consistent. They were uniform and covered the full target area of 25 cm^2. Rather than continuing in various other material systems, it then became the quest of this research to produce thin homogeneous metallic films from the pure vapor phase. None of the previous railgun system studies demonstrated this capability.

Through a series of screening and deflecting experiments, it was found that the plasma arc could be effectively moved about. With this as a basis, orthogonal rails were installed. The concept was that the vapor phase would undergo a 90 ° momentum change as a result of the Lorentz force. The heavier liquid droplets would be lost straight ahead, and thereby eliminated from the deposition. The simple 90° rails proved to be unsuccessful for this task. The rails were redesigned to a trapezoidal shape with increased breech height and width. These tapered rails successfully pulled the vapor phase and created a new thin film deposition technology.

The produced thin metallic films were generally between 100 - 200 nm thick. As the deposition process was additionally completed in less than 100 microseconds, the found structure was mostly very fine micro-crystalline. Grain sizes ran from 50 nm down to TEM resolution (approximately 2.5 nm). The system was also found capable of redeposition of metglas in the non-crystalline state. In fact, in the Al - Ti system internal carbon and oxygen was gathered by the deposition ions and due to the high quenching rate a metastable glass was formed. This glass

was formed on four consecutive shots. Additionally, a possible non-equilibrium metallic mixture in the crystalline state was identified. And finally, the system was found to be somewhat controllable in this mode of operation.

CHAPTER 6

CONCLUSIONS AND FUTURE RESEARCH

For simplicity, the conclusions and future research ideas are presented in point form.

CONCLUSIONS

1. Electromagnetic plasma acceleration by means of a railgun is an effective material transport means within a deposition system.

2. The detailed exploding foil device was an excellent source for plasma, vapor, and liquid deposition species.

3. Overall system versatility was greatly enhanced by having dual separate energy sources.

4. Although adequate for this and perhaps coating projects, a better evacuation system is needed for future thin film research.

5. Due to rail plating and erosion, a dedicated system which included matched material hardware would be superior.

6. The effects of high energy pulsed power on system components should be examined for the onset of the project. Elkonite, 67% W , 33 % Cu, proved to be a good candidate material.

7. To enhance energy input, system inductance could be further lowered by employing either substantial wire webbing or solid metal bus work.

8. This railgun deposition system proved most effective as a surface coating tool. Post treatments for surface truing may be required.

9. Coating adhesion was a function of energy input, material couple, and surface preparation.

10. Intermetallic compound formation is possible during the deposition process.

11. Immiscible materials and or alloys can be readily mixed at the sub-micron level using this technique.

12. The modified railgun system is capable of producing homogeneous thin metallic films.

13. Due to the microsecond deposition time scale and high quenching rate, ultrafine structure is obtained.

14. The modified system can also produce metallic based glasses.

15. The production of metastable and non-equilibrium thin films is too quite possible.

FUTURE STUDY POSSIBILITIES

1) Investigation of the effect of varying substrate temperature both heating and cooling. Heating should soften the surface for improvement in coating applications. Where cooling may enhance the quenching effect found during thin film production.

2) Consider the railgun and exploding foil devices as possible manufacturing tools for Rapidly Solidified Powders. Foil thickness and energy input could be used to control the liquid phase. Alloyed or multi-foils would serve as a means of composition control. Angularly adjusting rails might provide a means for size separation.

3) Given a good vacuum environment, experimentation with gas injection at triggering time to form nitrides and carbides. I would also suggest first backfilling and cleaning the deposition environment with a dry noble gas. Pre-shot surface sputtering could also be employed for high purity interface experimentation.

4) Similar experimentation using higher energy power sources, such as a quick pulse homopolar generator, or a compensating alternator, or multiple staged capacitance banks. This would allow for a much greater percentage production of vapor phase across the periodic table. The experiments could then be tailored for the system not around energy constraints.

5) Finally, development of an automated-continuously evacuated system for coating build up or increased area coverage. A system as such might also employ multiple guns and several element species for layered deposition.

APPENDIX ONE

SYSTEM HARDWARE

Figure A 1-1: Railgun deposition system; Capacitance discharge banks - right rear, and Deposition chamber - front left.

a)

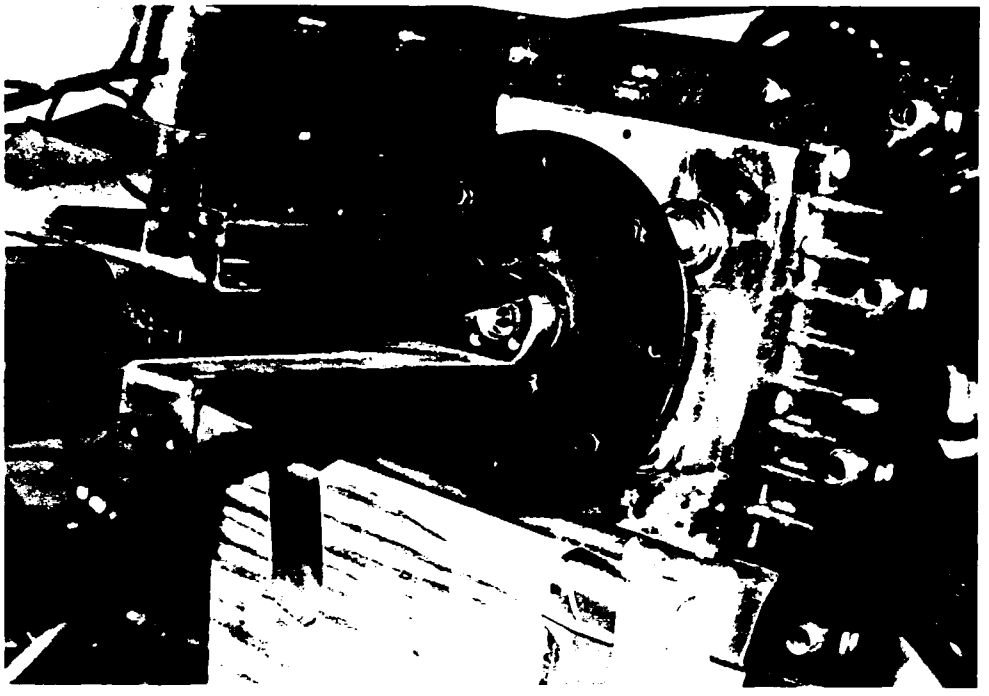

b)

Figure A 1 - 2: Square bore rails a) Coaxial configuration b) orthogonal configuration.

a)

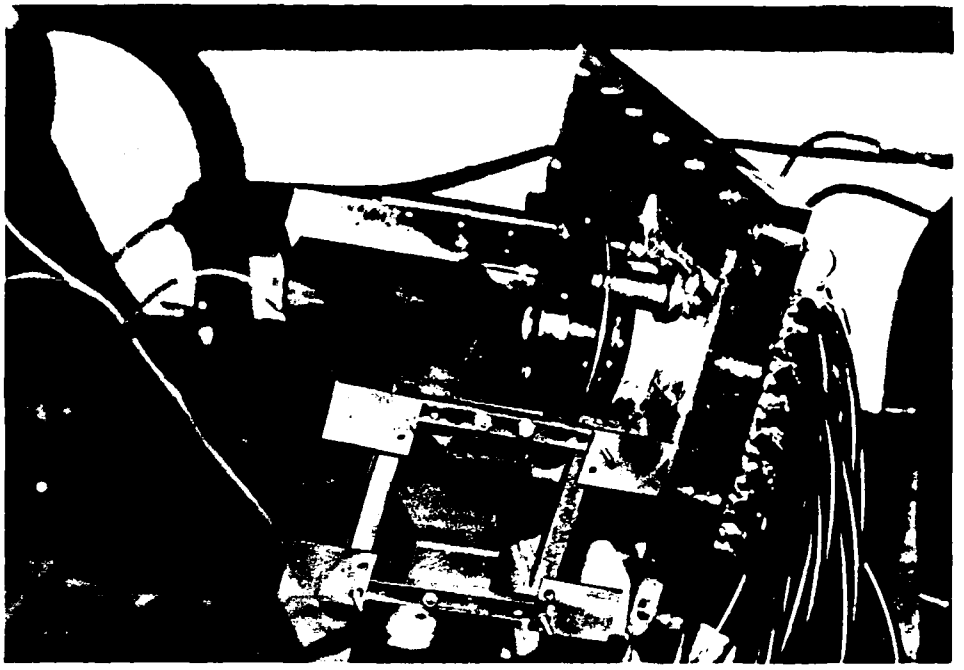

b)

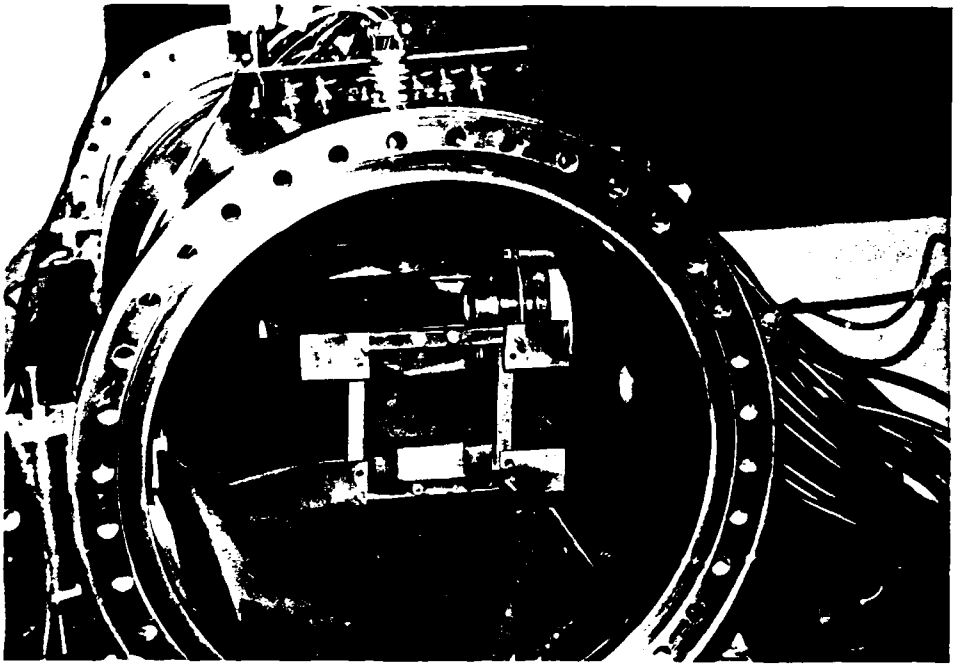

Figure A 1 - 3: Tapered Rails a) orthogonal configuration b) rails mounted within deposition chamber.

APPENDIX TWO
TAPERED RAIL SCHEMATIC

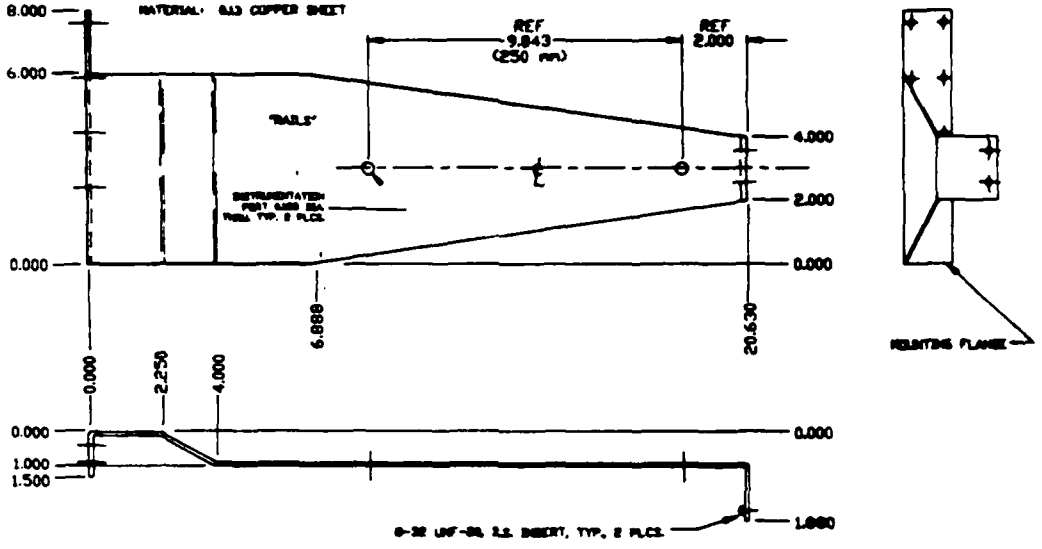

Figure A 2 - 1: Scaled drawing of the tapered rails.

BIBLIOGRAPHY

1. Bunshah, R. F., Deposition Technologies for Films and Coatings ,Noyes Publications, New Jersey. 1982.

2. Glang, R., Handbook of Thin Film Technology, McGraw Hill Inc. 1970.

3. Zaat, J. H., "A Quarter of a Century of Plasma Spraying," Annual Review of Materials Science, Volume 13, Annual Reviews Inc. Palo Alto, California, USA.1983.

4. Ashworth, V., Grant, W. A., Procter, R. P. M., Ion Implantation into Metals, Proceedings, 3rd International Conference on Modification of Surface Properties of Metals by Ion Implantation, Manchester, UK 1981, Pergamon Press Ltd, NY. 1982.

5. Matteson, S., Nicolet, M. A., "Ion Mixing," Annual Review of Materials Science ,Volume 13, Annual Reviews Inc. Palo Alto, California, USA. 1983.

6. Proceedings of the 3rd. Symposium on Electromagnetic Launch Technology '86, held in Austin TX. April 1986 IEEE Transactions on Magnetics, Vol. Mag-23, Nov. 1986.

7. Barber, J. P., Marshall, R. A., Rashleigh, S., "Magnetic Propulsion for a Hypervelocity Launcher," J. Appl. Phys. Vol. 49, 4 (April 1978) p. 2540.

8. Marton, L., Methods of Experimental Physics, Vol. 9. -Part B, Plasma Physics., Academic Press, New York. 1971.

9. Brast, D. E. and Sawle. D. R., "Feasibility Study for Development of a Hyper Velocity Gun," NASA-CR-60119 (1964).

10. Barber, J.P., "The Acceleration of Macroparticles in a Hypervelocity Electromagnetic Accelerator," Ph.D. Thesis, The Department of Engineering Physics, Australian National University, Canberra, Australia (1972).

11. Weldon, W. F., Woodson, H. H., Driga, M. D. "Compensated Pulsed Alternator," U. S. Patent 4,200,831 , 1977.

12. Hawk, R. S., Scudder, J. K., "Magnetic Propulsion Railguns: Their Design and Capabilities," in Megagauss Physics and Technology, ed. P. J. Turchi, Proceedings of an Int. Conf. on Megagauss Magnetic Field Generation and Related Topics, Washington, D. C. 1979.

13. Marshall, R.A., "Moving Contacts in Macro-Particle Accelerators", in High Power-High Energy Pulse Production and Application, ed. E.K. Inall, Australian National University Press, (Canberra) 1978.

14. Sokolowski, M., Sokolowski, A., Michalski, B., Gokieli, B., Romanowski, Z., Rusek, A., "Crystallization From a Reactive Pulse Plasma," Journal of Crystal Growth 42 pp. 507 - 511, North -Holland Publishing Company. 1979.

15. Osadin, B. A., Rusakov, N. V., "Condensation of an Erosion Plasma," Translated from Sov. Phys. Tech. Phys., Vol. 19, No. 2, August 1974, American Institute of Physics 1974.

16. Lau, J. H. W. and Margerun, J., "Application of Pulsed Plasma Acceleration in Thermal Spraying," Intl. Thermal Spraying Conference, 8th, Miami Beach, Florida, Sept. 1976.

17. Brown, L. D., "X-Ray, TEM, and Electrical Resistive Characterization of an FeBSi Glass," M.S. Thesis. The Department of Mechanical Engineering, Center for Materials Science, The University of Texas, Austin. Dec. 1983.

18. Spann, M. L., Brown, L. D., "Formation of Amorphous Metal by Hypervelocity Impact," EL-3238, Research Project 2115-6, Final Report, Oct 83, University of Texas, Austin.

19. Personal correspondence with CEM Staff members.

20. Honig, J., Kim, K., Wedge, S. W., "Hydrogen Pellet Acceleration With a Two-Stage System Consisting of a Gas Gun and a Fuseless Electromagnetic Railgun", J. Vac. Sci. Technol. A. Vol. 4, No. 3, May/June 1986.

21. Grevtsev, N. V. Kashurnikov, Y. M., "Motion and Condensation of Products from Electrically Exploded Wires," Moscow, Translated from Prikladnol Mekhaniki i Tekhnicheskoi Fizikt, No. 2, pp. 92-97. Feb 1974., Plenum Publishing Corp. New York. 1975.

22. Cook, R.W., "Obeservation and Analysis of Current Carrying Plasmas in a Railgun" Electromagnetic Launch Technology, 3rd Symposium Proceedings, April 1986, Institute of Electrical and Electronic Engineering, Inc., New York IEEE Transactions on Magnetics, Vol. MAG-23, Nov. 1986.

23. Azaroff, L. V., Elements of X-Ray Crystallography, McGraw-Hill Book Company, USA, 1968.

24. Goldstein, J.I., Newbury, D.E., Echlin, P., Joy, D.C., Fiori, C., Lifshin,E., Scanning Electron Microscopy and X-Ray Microanalysis, Plenum Press, New York. April 1984.

25. Thomas, G., Goringe, M. J., Transmission Electron Microscopy of Materials, John Wiley & Sons Inc. New York. 1979.

26. Finello, D., Marcus H. L., "Advances in and Quanification of Auger Electron Spectroscopy," Electron and Positron Spectroscopies in Materials Science and Engineering, ed.Buck, O., Tein, J. K., Marcus, H. L., Academic Press, Inc., New York, 1979.

27. Davis, L. E., MacDonald, N. C., Palmberg, P. W., Riach, G. E.,Weber,R. E., Handbook of Auger Electron Spectroscopy, Physical Electronics Industries, Inc., USA, Feb 1976.

28. Yushkov, V. I., "On the Problem of Selection of Conditions For Plasma Spraying," Svar. Proiz., 1976, No. 4 pp. 21-22.

29. Asinovskii, E. I., Zeigarnik, V. A., Kunavin, A. T., Matsenko, A. B., "Obtaining Copper Vapors With Pulsed Heating of Composite Conductors," Translated from Teplofizika Vysokikh, Temperature, Vol. 17, N0. 1, pp. 139 - 145, 1979, Plenum Pub. Corp. 1979.

30. Jager, H., Seydel, U., "Coatings of Metallic Surfaces by Electrical Explosions of Wires," Applied Physics, 2, pp. 345 - 347, 1973.

31. Sater, D. S., Gulino, D. A., Rutledge, S. K., "Coaxial Carbon Plasma Gun Deposition of Amorphous Carbon Films," NASA Technical Memorandum 83600, March 1984.

32. Aleksandrov, L. N., Dagman, E. I., Zelevinskaya, V. I., Petrosian, V. I., Skripkina, P. A., "Peculiarities of Formation and Properties of Semi-Conductor Films Deposited by Electrical Explosion," Thin Solid Films, 5 pp. 1-6, 1970.

33. Sokolowski, M., "Deposition of Wurtzite Type Boron Nitride Layers by Reactive Pulse Plasma Crystallization," Journal of Crystal Growth 46 pp. 136 -138, North Holland Publishing Company, 1979.

34. Sokolowski, M., Sokolowski, A., Gokieli, B., Michalski, B., Rusek, A., Romanowski, Z., "Reactive Pulse Plasma Crystallization of Diamond and Diamond-Like Carbon," Journal of Crystal Growth 47, pp. 421 - 426, North Holland Publishing Company, 1979.

35. Coudurier, L., Hopkins, D. W., Wilkomirsky, I., Fundamentals of Metallurgical Processes, International Series on Materials Science and Technology, Vol. 27, Pergamon Press,New York, 1978.

36. Rosebrock, T. L., Clingman, D. L., Gubbins, D. G., "Pulsed Electromagnetic Acceleration of Metal Plasmas," AIAA Journal, Vol. 2, No. 2, February 1964, pp. 328 - 334.

37. Harding, J. T., Kaplan, R. B., Pierson, H. O., Tuffias, R. H., Upshaw, J. L., "Chemically Vapor Depostied Materials For Railguns," Proceedings of the 3rd. Symposium on Electromagnetic Launch Technology '86, held in Austin TX. April 1986 IEEE Transactions on Magnetics, Vol. Mag-23, Nov. 1986.

38. Warne, M. A., "Application of Numerical Analysis Techniques," Cathodic Protection Theory and Practice, editors, Ashworth and Booker, Ellis Horwood Limited Pub. Chichester England, 1986.

39. Persad, C., Peterson, D. R., "High Energy Rate Modification of Surface Layers of Conductors," Proceedings of the 3rd. Symposium on Electromagnetic Launch Technology '86, held in Austin TX. April 1986 IEEE Transactions on Magnetics, Vol. Mag-23, Nov. 1986.

40. Walls, W. A., Weldon, W. F., Driga, M. D., Manifold, S. M., Woodson, H. H., Gully, J. H., "Improved Energy Density Homopolar Generator," Proceedings of the 3rd. Symposium on Electromagnetic Launch Technology '86, held in Austin TX. April 1986 IEEE Transactions on Magnetics, Vol. Mag-23, Nov. 1986.

41. Jackson, G. L., Farris, L.K., Tower, M. M., "Electromagnetic Railgun Extended-Life Bore Material Tests Results," Proceedings of the 3rd. Symposium on Electromagnetic Launch Technology '86, held in Austin TX. April 1986 IEEE Transactions on Magnetics, Vol. Mag-23, Nov. 1986.

42. Donaldson, A. L., Kristiansen, M., Watson, A., Zinsmeyer, K., Kristiansen E., Dethlefsen, R., "Electrode Erosion in High Current, High Energy Trabsient Arcs," Proceedings of the 3rd.Symposium on Electromagnetic Launch Technology '86, held in Austin TX. April 1986 IEEE Transactions on Magnetics, Vol. Mag-23, Nov. 1986.

43 Sokolowski, M., Sokolowski, A., Michalski, B., Romanowski, Z., Rusek, A., Wronikowski, M., "The Deposition of Thin Films of Materials With High Melting Points on Substrates at Room Temperature Using the Pulse Plasma Method," Thin Solid Films, 80 (1981) pp. 249 - 254.

44. Weber, F. N., Shear, D. D., "Exploding Wire Particle Size by Light Scattering Measurement," Journal of Applied Physics, Vol. 40 No. 9 August 1969, pp. 3854 - 3856.

45. Legresy, J. M., Audier, M., Simon, J. P., Guyot, P., "Crystallization Study of the Melt Spun AL-Fe-Si Glass," Acta Metallurgy, Vol. 34, No.9, pp. 1759 - 1769, 1986.

46. Megusar, J., Franks, G., Grant, N. J., "Development of a Ductile Crystalline Material from Co-Nb-B Metallic Glass," International Journal of Rapid Solidification, 1984-85, Vol. 1, pp. 291 - 303.

47. Tanner, L. E., Ray, R., "Phase Separation in Zr-Ti-Be Metallic Glasses," Scripta Metallurgica, Vol. 14, pp. 657 - 662, 1980.

48. Rajan, K., Sewell, P., "Intermediate Voltage Microscopy," Journal of Metals, December 1986, pp. 30 - 31.

49. Potter, D.I., Ahmed, M., Lamond, S., "Metallurgical Surfaces Produced by Ion Implantation," Journal of Metals, August 1983, pp.17 - 22.

VITA

Russell Joseph DeLuca [redacted] He is the proud son of Harold Joseph and Jessie W[redacted] DeLuca. After graduating with honors from General William T. Mitchell High School, Colorado Springs, Colorado, in 1974, he entered the United States Air Force Academy. As an undergraduate he studied Engineering Mechanics, and on 31 May 1978 was awarded the degree of Bachelor of Science with honors, and commissioned as an officer in the United States Air Force. On 7 July 1978 he married Kathye Jo Woodworth, and entered Undergraduate Pilot Training two weeks later. He graduated from Pilot Training on 22 June 1979. Over the next six years he served as an Operational Pilot and Instructor Pilot in the Air Force. During the summer of 1985, he was selected by The Air Force Institute of Technology to pursue an advanced degree in Engineering. In September, 1985, he entered the Graduate School of The University of Texas.

[redacted]

This thesis was typed by Russell J. DeLuca.